Borehole geophysical techniques to define stratigraphy, alteration and aquifers in basalt

Catherine M. Helm-Clark [a,b,*], David W. Rodgers [a], Richard P. Smith [b]

[a] Department of Geosciences, Idaho State University, Pocatello, ID 83209-8072, USA
[b] Idaho National Engineering and Environmental Laboratory, P.O. Box 1625, Mail Stop 2107, Idaho Falls, ID 83415, USA

Abstract

This paper concerns the interpretation of borehole geophysical data from basalt sequences, especially continental basalt sequences that host aquifers. Based on modifications of the rules used for interpreting borehole data from sedimentary rocks, new rules are proposed to identify the internal stratigraphy, aquifer boundaries, and alteration features in continental basalts.

The value of several wireline tools is critiqued. Natural gamma logs have limited utility in basalt sequences unless anomalously high-potassium or low-potassium basalt flows and/or sedimentary interbeds exist which can act as marker beds for stratigraphic correlations. Neutron logs can usually discriminate between individual flows, flow breaks and interbeds, even in unsaturated basalts. Neutron logs and temperature logs can also be used to map aquifer thickness in basalt. Gamma–gamma density logs are usually sensitive to the density contrasts between interbeds and basalt flows, and in combination with neutron and natural gamma logs are crucial for the correct interpretation of large void spaces in basalt such as collapsed lava tubes and formerly inflated pahoehoe lobes. Basalt porosity calculated from neutron, resistivity and/or gamma–gamma density logs is commonly overestimated due to the presence of hydrous alteration minerals. Velocity and resistivity logs are best at discriminating between flows in saturated conditions. Magnetic susceptibility logs may capture magnetic mineralogy variations at a finer scale than that of flows and flow breaks and therefore should always be interpreted in combination with other logs. Non-spectral neutron–gamma logs are not useful in basalt, though spectral neutron–gamma logs have been used successfully for stratigraphic correlation and to locate pollutants. Geochemical logs or the inclination of magnetic remanence provide the best data to discriminate individual flows with a basalt sequence, and thus establish an internal stratigraphy. Other tools used alone cannot provide reliable stratigraphic information, but a combination of tools may work. We recommend the combination of natural gamma, neutron, and gamma–gamma density logs in unsaturated rocks, and these logs plus velocity and resistivity logs in saturated rocks.
© 2003 Published by Elsevier B.V.

Keywords: Borehole geophysics; Basalt aquifers

* Corresponding author. Currently at: Idaho National Engineering and Environmental Laboratory, P.O. Box 1625, Mail Stop 2107, Idaho Falls, ID 83415, USA. Tel.: +1-208-526-4314; fax: +1-208-526-0875.

E-mail addresses: helmcath@isu.edu, helmcc@inel.gov (C.M. Helm-Clark), rodgdavi@isu.edu (D.W. Rodgers), rps3@inel.gov (R.P. Smith).

1. Introduction

Basalt stratigraphy has become an important issue in recent years because basalt sequences can host large aquifers. Extracting adequate water for consumption and agriculture while protecting the aqui-

fer from pollution requires a thorough understanding of basalt architecture. Accordingly, this paper reviews the utility of borehole geophysical tools in determining stratigraphic features of continental basalts. Much of this knowledge, the result of the abundant wireline data generated by the Deep Sea Drilling Program (DSDP), its successor, the Ocean Drilling Program (ODP) and the International Continental Drilling Program (ICDP), is relatively new or unknown outside of the marine geophysics community. Little of this data has crossed into other disciplines like geological engineering and hydrogeology, and a comprehensive interdisciplinary review of developments in wireline logging in basalt is clearly needed.

Wireline logging to establish basalt stratigraphy is usually difficult. The composition and texture of most basalts are rather uniform and many conventional geological and geophysical tools cannot discriminate their variation. This is especially true in continental flood basalts where thin but laterally extensive flows commonly display a uniformity of physical properties measured by conventional wireline tools (Crosby and Anderson, 1971). Furthermore, wireline responses in basalt can vary greatly depending on whether logging conditions are saturated or unsaturated. Most borehole geophysical surveys in basalt have been conducted where the basalt was saturated with drilling mud, saltwater, or fresh water. This has been the case for all oceanic basalts (Goldberg, 1997; Becker et al., 1989) and for many continental flood basalts like the Deccan Traps in India which host shallow unconfined aquifers (Buckley and Oliver, 1990; Versey and Singh, 1982; C. Cheney, pers. comm.). There are few wireline studies in unsaturated basalts (Crosby and Anderson, 1971; cf. Last and Horton, 2000). One exception is the geophysical logging program at the Idaho National Engineering and Environmental Laboratory (INEEL), which has generated perhaps the largest collection of wireline logs for continental basalts in both saturated and unsaturated conditions. We have mined the INEEL Hydrogeological Data Repository (HDR) extensively for examples used in this paper.

This paper will demonstrate the value and the pitfalls of wireline logging in continental basalt. The data and results are derived from published investigations of basalt from the Deccan Traps of India, the Karoo Flood Basalts in Botswana, the island of Hawaii, the New Jersey/Connecticut Triassic Rift Basin, the Columbia River Plateau, and the Eastern Snake River Plain. While Hawaii and similar intraplate islands are not technically continental, we include them here since the layered nature of large oceanic-island shield volcanoes closely resembles that of continental flood basalts. We begin by describing the range of continental basalt textures, and then show how different wireline tools may record these variations. The goal is to derive a valid set of interpretive rules for logging basalts in a wide variety of continental settings. Some DSDP and ODP results are also discussed to help refine on-land interpretation; to learn more about oceanic borehole geophysics in basalt, the reader is referred to the fine review papers by Goldberg (1997) and Brewer et al. (1998).

2. Basalt types and morphologies

A basalt can be classified by its composition, texture, and magnetic character and distinguished from other basalts by variations in these properties. Compositional and magnetic variations are described in later sections but textural properties such as flow thickness, fracture patterns, and the nature of vertical sequences are so important to wireline interpretation that they are described in more detail here.

The most common morphologic type of basalt is pahoehoe lava (Ehlers and Blatt, 1982; Macdonald, 1972). Pahoehoe flows are typically vesicular and fractured at their top and bottom boundaries, but massive in their centers. Flow tops and bottoms can be cindery or scoriaceous. The top of a pahoehoe flow commonly forms a solid ropey rind under which magma can travel great distances, either as sheet flow or through lava tubes. Flow bottoms are commonly oxidized and flow tops may be glassy. In contrast, the interiors of flows cool more slowly than the margins, resulting in larger grain sizes, little to no vesicles, and few to no fractures.

Pahoehoe flows can vary from less than 3 m to as much as 50 m thick, regardless of horizontal extent. Typically, an erupting flow will form a hummocky surface whose undulations can have amplitudes from 1 to 15 m. The lateral extent of pahoehoe is highly variable, with some flows extending less than 1 km from their vents, like those on the Snake River Plain

(Hughes et al., 1999); others extending tens of kilometers, like on Hawaii (Stolper et al., 1996); and some extending for over 500 km, like the basalt flows of the Deccan Traps (Versey and Singh, 1982).

Pahoehoe can erupt from the vents of shield volcanoes or from fissures. Close to a vent, scoria, cinders, and very thinly bedded (<2 m) shelly pahoehoe are not uncommon (e.g., Greeley and King, 1975; Sharp, 1976). Along the leading edge of an erupting flow, lobes of pahoehoe become inflated with magma which can break out to form more hummocky lobes, thus expanding the flow area (e.g., Hughes et al., 1999). Between the eruptive vent or fissure and the advancing flow front, basaltic magma typically travels through conduits such as lava tubes and inflated lobes (Greeley, 1982a; Macdonald, 1972). These conduit features will eventually collapse, creating cavity-rich basalt rubble. Substantial talus and sedimentary material can accumulate in these feature both before and after collapse (Greeley, 1982b).

In contrast to pahoehoe flows, the less-common aa flows are characterized by rubbly flow fronts and rubbly-to-blocky flow tops (Ehlers and Blatt, 1982). Typically, aa is less vesicular than pahoehoe and is laterally limited. Some pahoehoes grade into aa at their flow fronts as a result of degassing and increased
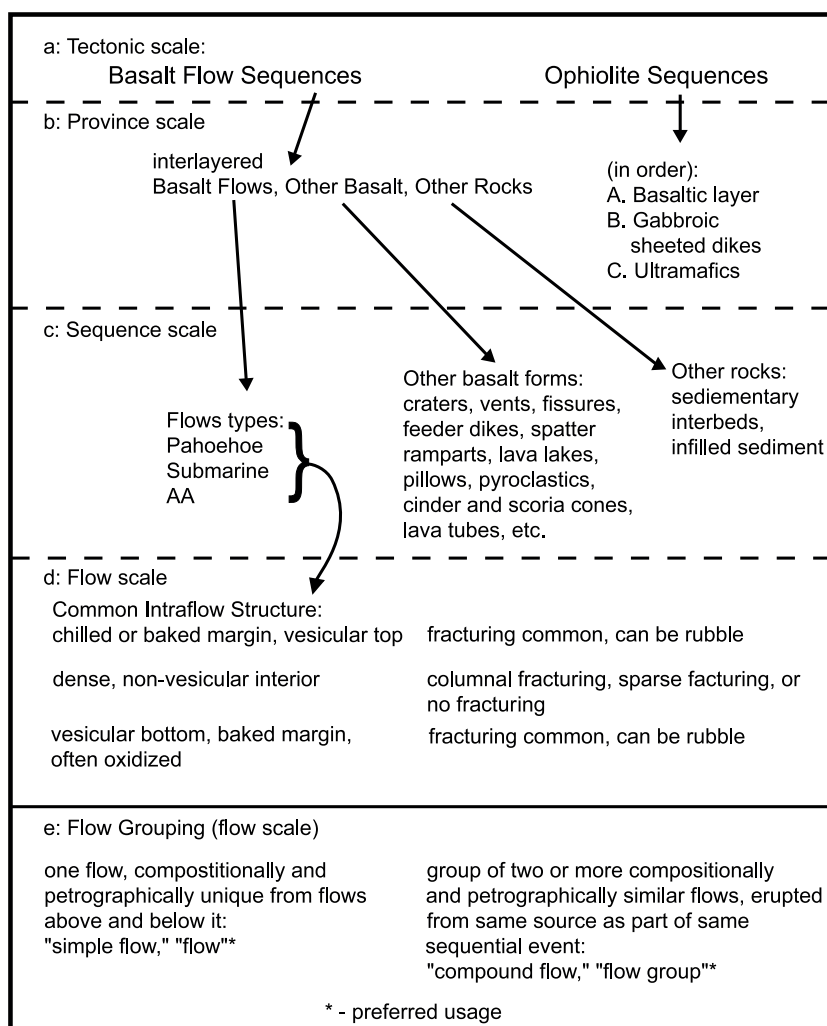

Fig. 1. A simplified hierarchy of basalt features at several scales.

viscosity from cooling. Other aa flows erupt directly, as they do on Iceland (Macdonald, 1972).

Most pillow basalts form on the ocean floor (Anderson et al., 1982) but rarely in continental basalt flow sequences. Because of their comparative rarity on land, we do not discuss pillow basalts in this study, but refer the reader to the work of Haggas et al. (2002), Brewer et al. (1998), and Brewer et al. (1990), as well as to the copious literature of the DSDP and ODP.

In all basalts, cracks and fractures become the sites of secondary mineral growth. Alteration typically starts near flow margins and works inward (Cheney, 1981). Common secondary minerals include calcite, clays, and/or zeolites. Vesicles are also sites of secondary mineral growth and alteration, like the abundant amygdales of the Deccan Traps (Buckley and Oliver, 1990). Younger basalts are more likely to host unaltered and unfilled vesicles than older ones. For all basalt flows, post-emplacement erosion and soil development can both destroy flow surfaces and cause rubble formation at the tops of flows. Depending on the time elapsed between basalt eruptions, a sedimentary interbed or "intertrappean" layer may develop and be preserved in the geologic record. Examples include beach sediments as interbeds on Hawaii (Beeson et al., 1996), and loess sediment interbeds on the windswept East Snake River Plain (Hughes et al., 1999; Blair, 2002).

Most basalt occurs not as individual layers but as thick sequences of lava flows with sedimentary interbeds. Flows can be either simple or complex (Walker, 1972) (see Fig. 1). Simple flows are compositionally

Table 1
Tectonic classification of basalt

Tectonics	Size	Composition	Principal minerals	Common morphological features	Examples
Oceanic spreading centers and ocean floor					
Divergent boundary between two oceanic plates	70% of the Earth's surface	Mid-Ocean Ridge Basalts (MORB), mostly olivine tholeiites, low K, low Ti; often pervasively serpentinized	Olivine, calcium-rich plagioclase	Ophiolites: pillow basalts, shallow dikes and sills, gabbroic sheeted dikes, basal ultramafics	East Pacific Rise, California Coast Range Ophiolite
Oceanic island chains and plateaus					
Intraplate, thought to be fed by mantle plume	Variable	Ocean Island Basalts (OIB): tholeiite and occasional late alkali basalt; enriched in K, Th and U with respect to MORB	Tholeiite: calcium-rich plagioclase, pyroxene, commonly olivine. Alkali: olivine, feldspathoids	Large shield volcanoes, hyaloclastites, pillow basalt, linear rifts and fissures, lava tubes, compound flows of pahoehoe and aa	Hawaii, Reunion
Continental flood basalts					
Intraplate, extensional regime, continental rift or mantle plume	>100,000 km^3 ("flood basalt")	Continental Flood Basalts (CFB): tholeiites, andesitic basalts, typically richer in Si and K than MORB	Clinopyroxene, plagioclase	Mostly laterally extensive pahoehoe sheets, compound flows close to vents, simple flows distally; pillow and palagonite complexes	Karoo Flood Basalts, Deccan Traps, Columbia River Plateau
Continental volcanic fields					
Intraplate, extensional regimes; ("plains basalts"; basin and range volcanism)	<100,000 km^3	A large variety of basaltic and andesitic rocks, often associated with bimodal volcanism	Clinopyroxene, plagioclase, and/or olivine; feldspathoids in alkali basalts	Small low-angle shields, lava tubes and vents feeding surface flows; laterally limited, simple and compound flows; small cinder and scoria cones	East Snake River Plain (ESRP), Clear Lake Volcanic Field

unrelated to the flows immediately above and below them. They have a discernable top, middle, and bottom, and their geochemistry and petrography are distinct. Compound flows are clusters of flow units all sharing the same geochemical and petrographic features. This uniformity of physical properties suggests strongly they were erupted from the same source in a short period of time. The flow units in a compound flow usually have a preserved flow top to distinguish them from other flow units. There should be little to no soil or sediment separating each flow unit. In some basalt provinces, e.g., the Deccan Traps, a flow may be compound near its vent and a simple flow at distance (Versey and Singh, 1982). When using wireline tools in a borehole, it may be impossible to determine if a flow is a simple flow or an individual flow unit of a compound flow, depending on the choice of wireline tools used. For this reason, some researchers prefer to use the terms flow groups and flows instead of compound flows and flow units (e.g., Kuntz et al., 1980; Anderson and Lewis, 1989). For convenience, this is the usage we prefer and will use for the remainder of this paper.

Different basalt compositions occur in different tectonic environments, and those environments commonly exert a controlling influence on the morphology of basalt. It is useful exercise, therefore, to classify basalt by tectonic environment (see Table 1). If we know how tectonic environment influences basalt, then we will have a preliminary idea of what to expect during drilling and wireline logging. For example, geothermal exploration near The Geysers geothermal field might encounter the pillow basalts of the California Coast Range ophiolite (Bailey et al., 1964). In comparison, ground water investigations on the Columbia River Plateau will likely encounter the 500-km-long, ~ 50-m-thick Grande Ronde flow of the Columbia River flood basalts (Hooper, 1997).

3. Wireline logging of basalt

Having outlined the common features of basalt morphology which can be used to describe the stratigraphy of a basalt flow sequence, we need to examine the wireline tools which can measure these and other stratigraphic features. We classify stratigraphic features as either primary or secondary. Pri-

mary features are those intrinsic to the basalt itself, such as composition or vesicularity. Secondary features are not intrinsic; however, they are related in some way to basalt and are useful in establishing stratigraphy, e.g., the presence of interbeds or saturated vs. unsaturated conditions.

In the description of wireline tools which follows, we describe the basis of each tool, its application to basalt, and potential problems of interpretation in basalt. Not all logs are discussed. Some, like the caliper log, are so straightforward that discussion is deemed unnecessary. Other logs, like flowmeters, behave the same regardless of the rock type. Some tools like nuclear magnetic resonance are relatively new and have little to no track record yet in basalt. Some tools are so specialized that they have little application to basalt. Much of the discussion concerns tool categories, not specific tools. For example, resistivity is one of several tool categories, whereas laterologs, point resistance, and induction tools are specific tools in that category.

4. Natural gamma logs

Three naturally occurring radioisotopes have decay chains and modes involving the emission of gamma rays, specifically ^{40}K; ^{238}U and its daughter products; plus ^{232}Th and its daughter products. The energy spectrum of these decays is concentrated between 0.2 and 3.0 MeV. A natural gamma log records total decay events across the gamma energy spectrum. Most modern natural gamma results are reported in API units (Belknap et al., 1960; Keys, 1990). A variation of the natural gamma log is the spectral gamma log, which discriminates the contribution of different parts of the gamma energy spectrum (Schlumberger Wireline and Testing, 1989). Since K, Th, and U contribute to different parts of the gamma energy spectrum, this information can be used to determine the concentration of each of these elements, respectively.

5. Natural gamma logs—basalt applications

The natural gamma log is sensitive to several stratigraphic characteristics in basalt, the most impor-

tant of which is anomalous potassium content in basalt and clayey interbeds. Basalts have very low potassium, uranium, and thorium concentrations, where potassium content usually dominates the natural gamma signature (e.g., Hughes et al., 2002; Anderson and Bartholomay, 1995; Versey and Singh, 1982). Natural gamma counts for a basalt are typically between 5 and 50 API.

Variable potassium content can sometimes be used as a primary stratigraphic feature in basalt. The composition of basalt is commonly uniform within a basalt province and there is little variation in K concentration, e.g., the Karoo flood basalt remnant exposed in Botswana (Cheney, 1981; Cheney and Farr, 1980). In other basalt provinces, however, anomalously high or low K-content basalt flows exist in the subsurface, and these flows can be used as marker beds for establishing stratigraphic correlations, e.g., the Deccan Traps (Buckley and Oliver, 1990).

An important secondary stratigraphic feature is the clay content of sedimentary interbeds. Sedimentary interbeds commonly contain higher levels of potassium, uranium, and/or thorium than the flows themselves. This is mainly due to lithological differences, most notably the presence of clays and other phyllo-

silicates minerals which have intrinsically higher radioisotope content than basalt (Buckley and Oliver, 1990).

6. Natural gamma logs—results and interpretations

Natural gamma logs may be used for correlating basalt flows between boreholes if high-gamma emitting interbeds and/or anomalously high- or low-gamma emitting basalt flows are present. Fig. 2 is a cross section through the Deccan Traps in the Betwa Basin in central India, showing an anomalously high gamma-emitting basalt with respect to its neighbors (labeled A on Fig. 2). Evidence from lithological logs and geochemical analyses of subsurface samples demonstrates that a handful of Betwa Basin flows are consistently higher in natural gamma emissions when compared to most other flows (Versey and Singh, 1982). These higher-potassium flows do not show lateral variation in their total natural gamma measurements, even when traced over tens of kilometers. Using geochemical measurements, Versey and Singh (1982) determined that the high-gamma flows had ~ 4 times the K_2O and
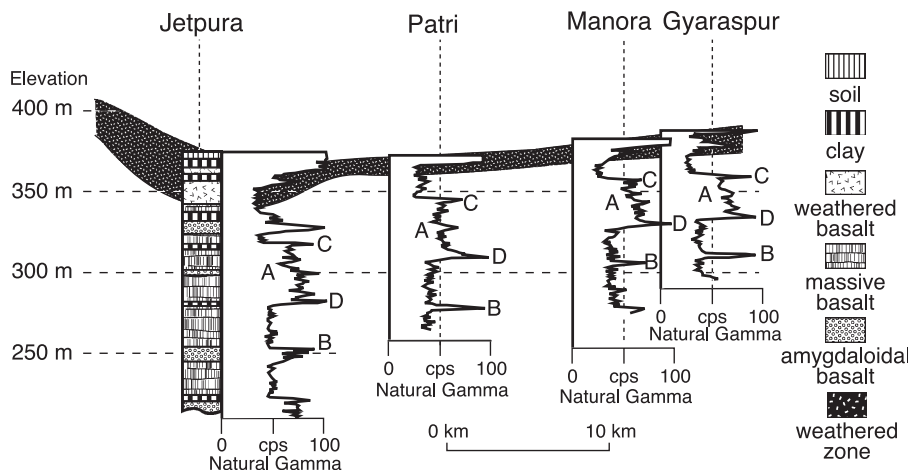

Fig. 2. The natural gamma logs shown here are for boreholes in the Deccan Trap flood basalts in central India. Log data was collected in saturated conditions. Natural gamma counts increase to the right in this figure. Geology and log interpretations are based on Versey and Singh (1982) and Buckley and Oliver (1990), who used lithological logs and geochemical analyses to define their stratigraphy. The ~ 50-m-thick high-natural-gamma-count basalt is a marker bed (labeled A) which can be traced over 50 km. The narrow spike (labeled B) below the 50-m-thick basalt is not an interbed, but an altered amygdaloidal basalt flow. The "horns" labeled C and D at the top and bottom of the high-natural-gamma basalt layer A correspond to clay beds. This figure is modified from Buckley and Oliver (1990).

2 to 3 times the Th content compared to the majority of other local flows, thus demonstrating that the increased gamma emissions are due to differences in the basalts themselves, and not due to the presence of amygdales or secondary alteration minerals. These characteristics make it possible to use this and similar high-gamma flows as marker beds, enabling correlations of flows over distances as great as 100 km (Buckley and Oliver, 1990; Versey and Singh, 1982).

Fig. 3 shows a cross section through the Eastern Snake River Plain. The logs shown here were collected over a 50-year period using a variety of wireline tools, so the results are relative and qualitative only. Even so, the interpretation of these logs is based on comparison with the continuously collected cores from three deep boreholes along or near this cross section. Several features on the logs can be therefore correlated between wells with confidence. In Fig. 3, the high-gamma count interbed labeled "A" pinches out to the north as it gains in elevation, a behavior observed in present-day loess deposited on the sides of volcanic cones at nearby Craters of the Moon National Monument. Feature B is the flow boundary between a low-K flow group above and a higher-K flow group below, making this feature a usable stratigraphic marker. Feature C in Fig. 3 is a pair of interbeds. The top interbed shows variable thickness which apparently pinches out to the south.
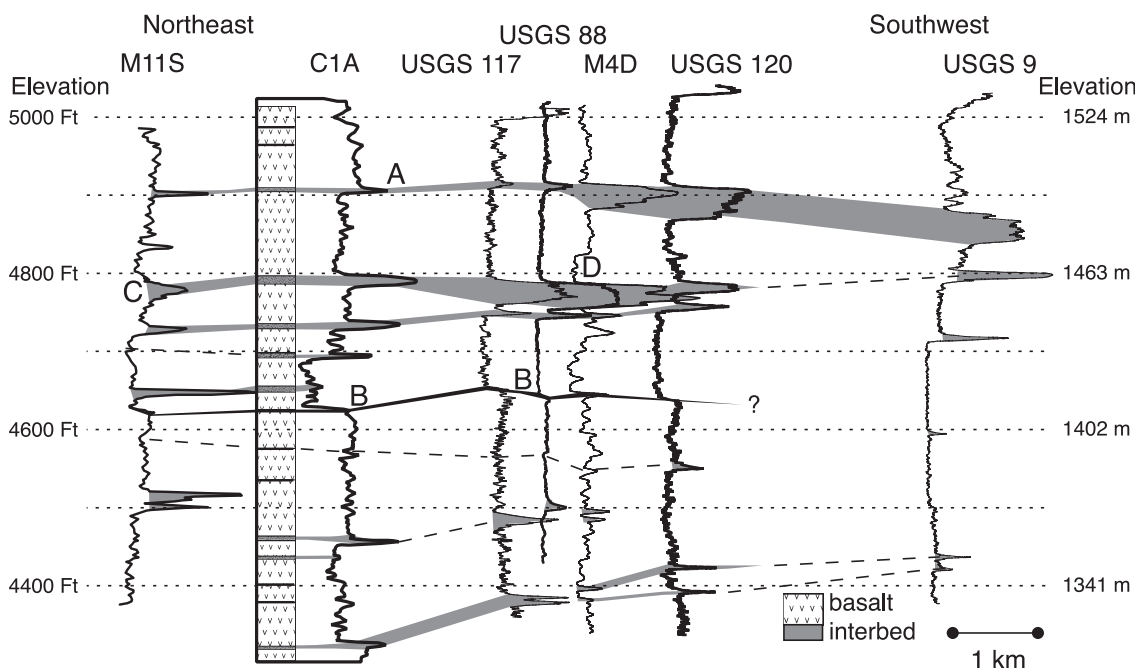

Fig. 3. Twelve-kilometer natural gamma cross section of wells on the Eastern Snake River Plain. Natural gamma counts increase to the right. The staggered vertical positions of the logs correspond to their relative elevations in the field. Logs were collected over a 50-year period using six generations of wireline tools and reporting results in three different units of measure. All log results shown here should be considered qualitative only. Interpretations are in part based on thin sections and core-to-log correlations for wells BG 77-1, USGS-118 and C1A at the Idaho National Engineering and Environmental Laboratory (INEEL) (Barraclough et al., 1976; Kuntz et al., 1980; Anderson and Lewis, 1989; Knutson et al., 1994; Anderson and Bartholomay, 1995; Blair, 2002; and unpubl. data archived at the INEEL HDR by Knutson, 1993–1994, and Helm-Clark, 2001–2002). These three wells are along or within 1 km of the cross section shown. A composite lithological log is shown here for well C1A. The stratigraphic interpretation is that of the authors. Shaded units are interbeds or flow breaks. Dotted lines are inferred flow boundaries. Features: A—high-natural-gamma-count interbed correlated in most of the wells; B—flow boundary between a low-K flow group above and a higher-K flow group below, suitable as a stratigraphic marker; C—pair of high-natural-gamma-count interbeds correlated across several wells; D—possible collapsed structure.

7. Natural gamma logs—potential problems of interpretation

There are several factors which can lead to the misinterpretation of natural gamma logs in basalt. A common one is the lack of recognition of textural features. For example, feature D in Fig. 3 has the appearance of a low-K flow which has no correlatives in nearby wells. In fact, the wells to the north (USGS-88, USGS-117) lack this feature and the nearest well to the south (USGS-120) shows slightly elevated gamma counts at the corresponding position to feature D. Since the spacing between these wells is a kilometer or less, it is unlikely that a localized K-poor flow was erupted into such a small area. Alternatively, it is possible that the low gamma counts at D are due to a localized morphological phenomenon such as a col-lapsed lava tube, a formerly inflated pahoehoe lobe, or other void-rich feature. Pahoehoe can accommodate many void spaces. Overlying flows do not necessarily fill all the voids in flows underneath, so large voids spaces can and will occur in the subsurface (Welhan et al., 2002). Voids do not contribute any gamma decays and so will yield anomalously low natural gamma counts. Where there are no correlative low-gamma layers in nearby wells, increased void spaces should be suspected and can be confirmed by collecting a density log. Void morphology is discussed in more detail in the section on gamma–gamma density logs.

Interbedded sediments are not always associated with elevated gamma counts. For example, Buckley and Oliver (1990) reported a diatomite interbed in the Deccan Traps which emitted a low gamma flux and therefore had low contrast with respect to basalt. In this case, the natural gamma log could not discrimi-nate between the diatomite and basalt flows above and below it.

Groundwater will attenuate measured gamma counts in holes greater than ~ 15 cm (6 in.), assuming that the borehole contains no drilling fluid at the time it is logged (Crosby and Anderson, 1971). The larger the hole the greater the attenuation. While this is an effect that can be seen in any type of strata, it is particularly pronounced in basalt where total gamma emissions are small and counting statistics are less favorable than in other rock types. For stratigraphic interpretation, quantitative measurement of potassium content is possible if the tool is properly calibrated and all the necessary corrections have been made for the presence of drilling mud, water, casing, and/or borehole diameter. Without such corrections, quanti-tative correlations are impossible. Qualitative correla-tions can still be made, however, if anomalous gamma-count layers exist in the subsurface.

8. Neutron logs

All neutron tools employ a source of fast neutrons (>0.1 MeV). The effects of neutron interactions with borehole fluids, pore-space fluids, and rock matrix are subsequently measured with a variety of detectors and detector geometries. A useful parameter integral to the arrangement of detectors is the slowing-down length, L_s. L_s is the root-mean-squared distance that a fast neutron must travel before it is thermalized, i.e., before reaching the thermal energy range of < 0.1 eV (Schlumberger Wireline and Testing, 1989). Slowing-down length is a function of the bulk density, the concentration of neutron moderators, and the scattering and capture cross sections of those moderators (Broglia and Ellis, 1990). When hydrogen is present, its L_s will dominate all others due to its very large scattering and capture cross sections. For example, L_s in water is much shorter than L_s in calcite, despite the fact that calcite is the denser material. Other elements with large neutron capture cross sections like chlorine may also shorten L_s, e.g., connate brine vs. potable water. In reality, how-ever, this effect is small and is rarely observed, even when crossing a fresh-to-saline water interface (Keys, 1990).

Neutron logs are usually named for what they detect. A neutron–epithermal neutron log detects neutrons in the epithermal 0.1 to 100 eV range where the detector is at a distance greater than L_s from the source. At this distance, the epithermal neutron flux will decrease as an increasing number of neutrons are thermalized. Since there are few elements that can moderate neutron flux as well as hydrogen, the flux decrease is mainly due to an increase in hydrogen content, usually with a logarithmic proportionality. A neutron–thermal neutron log operates the same way as the epithermal log, except the detector measures neutron flux in the < 0.1 eV range. In the thermal energy range (< 0.1 eV), hydrogen does not moderate thermalized neutrons, but will prefer to capture them

instead. An often-used variation in neutron logging is to place the detector at a distance less than L_s from the source. In this case, the detected epithermal or thermal neutron flux will be linearly proportional to hydrogen content. This is the basis of the moisture meter which is most often used in soils and the unsaturated zone.

The traditional interpretation for neutron logs in saturated rocks assumes a negative correlation between water content in interconnected pore spaces and the thermal or epithermal neutron counting rate; these results can be converted into a porosity measurement if a material-specific calibration exists (Broglia and Ellis, 1990). In contrast, in unsaturated conditions, traditional neutron tools and moisture meters do not measure porosity per se, but rather are assumed to measure any moisture in the rock's pore spaces (Crosby and Anderson, 1971).

9. Neutron logs—basalt applications

Neutron logs can discriminate features in basalt such as flow breaks, fracture zones, alteration, inter-

beds, and aquifer thickness. For example, decreased neutron flux at flow breaks can help determine stratigraphic details (Crosby and Anderson, 1971; Siems, 1973). Sharp decreases in neutron flux also correlate to increased fracture porosity and other permeable zones when in saturated basalt. In the unsaturated zone, flow breaks, fractures, and other permeable intervals in basalt will correspond to decreased neutron flux if they host increased moisture, perched ground water, or hydrous alteration minerals. Neutron logging may also distinguish secondary stratigraphic features such as sedimentary interbeds if water or hydrous minerals are present. For example, a hydrogen-rich clay will affect the neutron flux, but an unsaturated quartz arenite will not.

10. Neutron logs—results and interpretations

Fig. 4 shows epithermal neutron logs and stratigraphic correlations from the Columbia River Plateau flood basalts (Siems, 1973). These logs are qualitative and neutron flux increases to the right. Flow groups and
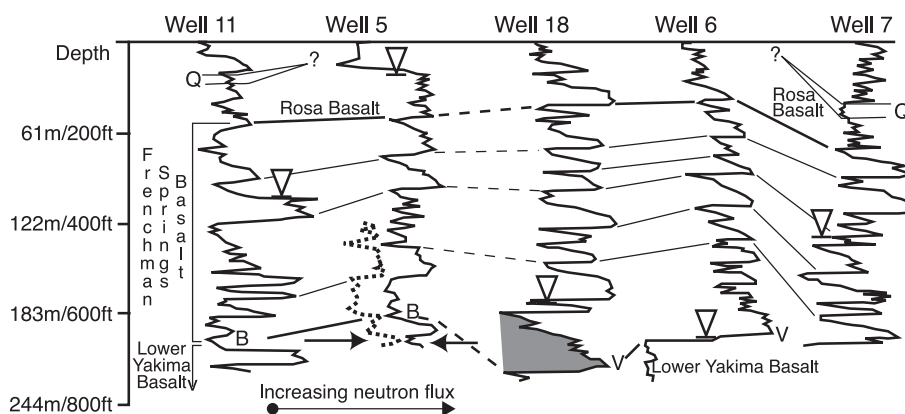

Fig. 4. Neutron cross section of wells on the Columbia River Plateau in northeast Washington State. Neutron counts increase to the right, unsaturated zone moisture/saturated porosity increases to the left. Unfortunately, all the logs from Siems (1973) were presented as qualitative data with no units of measure reported, so scale and units are not known for these logs. Black arrowheads mark the top of the unconfined aquifer. Siems (1973) recorded neutron logs at different scales above and below the water table, and spliced the data together at the water table for presentation. Black lines are correlations by Siems (1973). Dotted lines are inferred correlations. Vertical arrowheads mark the top of the water table. Feature Q is the Quincy diatomite. Feature V is the Vantage sandstone. Feature B is a blue clay/siltstone. The traverse is ~40 km long, though the spacing shown between wells is not to scale. The dotted line to the left of the neutron log for well 5 is a portion of the natural gamma log for this well. Horizontal arrows mark the location of a possible clay-rich layer, based on increased natural gamma counts plus decreased neutron counts. A known clayey layer in well 5 is the blue clay/siltstone labeled "B" just above the arrows, again where natural gamma counts increase as neutron counts decrease. The lack of the expected drop in neutron counts at the water table for wells 11 and 5 is due to the scale change in the recorded data at the water table (Siems, 1973). Wells 18, 6 and 7 do show an overall drop in average neutron counts at the water table. In wells 18 and 7, the drop is subtle, unlike well 6, where it is very abrupt. This figure is modified from Siems (1973).

other strata were identified by Siems (1973) using lithological logs, petrographic and geochemical analyses of cuttings, exposures of correlative flows in nearby deeply cut river canyons, natural gamma logs, and epithermal neutron logs. Siems (1973) identified the Quincy diatomite (labeled "Q" on Fig. 4), the Ventura sandstone (labeled "V"), and a variably lithified blue clay/siltstone (labeled "B") as interbeds in these and several other wells in western Washington State. Based on lithological logs and geochemical data, Siems (1973) correlated flow breaks with sharp decreases in neutron flux on Fig. 4, and attributed the change in flux due to increased porosity, higher water content, and/or the presence of clays and other hydrous minerals.

Neutrons detected, counts per second

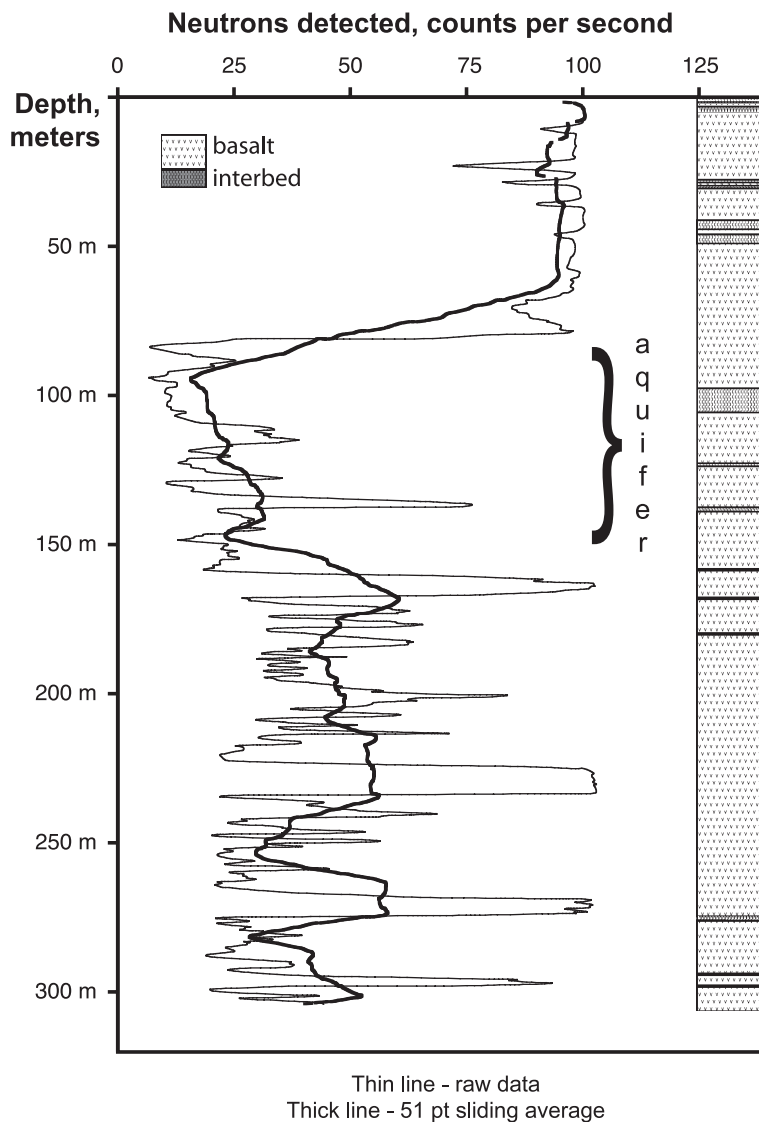Thin line - raw data
Thick line - 51 pt sliding average

Fig. 5. Neutron counts for well USGS-30 on the Eastern Snake River Plain. Stratigraphic column from Chase et al. (1964). Thin line—neutron counting rate data. Thick line–sliding average of 51 data points to show more clearly the regions of high, low and moderate average neutron flux in the well. Unattenuated high neutron counts in unsaturated basalt are obvious above the water table. Neutron counts are lowest in the aquifer layer. Moderate neutron counts below the aquifer are interpreted as the attenuation of neutron flux by hydrous alteration minerals.

A portion of the natural gamma log (the dotted log trace) from well 5 is also shown in Fig. 4, next to its epithermal neutron log. The signature of hydrous minerals on this log is manifest as increasing natural gamma vs. decreasing neutron counts at two depths near the bottom of well 5. Between the arrows, the presence of hydrous minerals associated with converging gamma and neutron peaks is conjectural. Above the arrows, however, increasing natural gamma vs. decreasing neutron counts correlate with the blue clay/siltstone at feature B.

An interesting textural feature on the Columbia River Basalt logs is an overall top-to-bottom increase in the neutron flux for many flows (e.g., shaded area, well 18, Fig. 4). Siems (1973) attributed this effect to decreasing porosity from the flow top to the massive interior of each flow. Similar behavior has also been observed in saturated subsurface basalt flows on the Eastern Snake River Plain, several of which occur in INEEL boreholes including well C1A. For C1A, an increase in neutron flux is only loosely correlated with a decrease in porosity from the top to the bottom of flows (J.C. Crocker, 1992, unpubl. data archived at the INEEL HDR). C1A porosity measurements on cores, however, do not account for any fractures present in basalt flows. Based on examination of C1A cores, fractures are most prevalent at the tops of basalt flows (Helm-Clark, unpubl. data), and most of the permeable zones in the local aquifer are associated with this fracture-based porosity (Welhan et al., 2002). If the porosity measurements on core and the observed fracture trends of flows are both considered, then Siems's correlation of increasing neutron flux vs. decreasing porosity in saturated basalt flows appears to be true.

Since altered basalts can sometimes be traced over large distances in some basaltic provinces (e.g., the Deccan Traps, bed B, Fig. 2), coherent zones of alteration may be used for stratigraphic correlations. For example, using geochemical analyses of cores, Morse and McCurry (1997, 2002) showed that the bottom of the Snake River Aquifer corresponds to the top of a widespread basalt alteration zone, with authigenic minerals filling fractures, cracks, and vesicles. This alteration horizon is present in every cored well at the INEEL, spread over an area greater than 1000 km^2. Such an alteration zone should be evident on INEEL epithermal neutron logs compared to unsaturated basalt, since L_s in altered basalt will be shortened by the addition of chemically bound hydrogen in clays and other hydrous alteration minerals.

Fig. 5 shows the epithermal neutron log for well USGS-30 at the INEEL. The top of the aquifer stands out as the steep decrease in neutron counts at ∼ 80 m below land surface (bls). The bottom of the aquifer is at ∼ 160 m bls, where neutron counts increase from very low average values to higher average values. These picks for the top and the bottom of the aquifer agree with the aquifer boundaries mapped by temperature logging in this well (Smith et al., 2002). Based on Morse and McCurry (2002), the bottom of the aquifer also corresponds to the top of the altered basalts. Compared to the unsaturated and unaltered basalts above 80 m bls, the neutron counts for the basalts below 160 m bls are moderate to low. Since the growth of authigenic minerals in fractures and other void spaces will reduce and eventually eliminate porosity, it is safe to assume that there is little free water in the subaquifer basalts. This strongly suggests that the neutron flux below the aquifer is due to the growth of hydrous alteration minerals, as Morse and McCurry (1997) suggested.

11. Neutron logs—potential problems of interpretation

Morin et al. (1993) investigated the behavior of different source-to-detector spacings when logging in unsaturated basalt with conventional neutron logging tools. They found that for all but the widest separation, their tool behaved like a moisture meter in the unsaturated zone, and not like a conventional neutron log. The spacing at which the tool began to behave like a standard neutron log (>1 m) was also far enough that the neutron flux was very low. They concluded that to prevent marginal counting statistics at large source-to-detector separation, the logging rate should be decreased or a stronger neutron source employed. The implication of this experiment is that conventional neutron logs in unsaturated basalt should be interpreted with caution, especially if the tool used has a source-to-detector spacing of under a meter.

Using neutron log results to calculate porosity in basalt is difficult. The first impediment is that most neutron tools are calibrated for sedimentary rocks. Even if a basalt-specific calibration exists, the experi-

ences of the DSDP, ODP (Broglia and Ellis, 1990), Mt. Hood Geothermal Project (Blackwell et al., 1982), and other logging projects in basalt (Knutson et al., 1994) show that neutron data does not correlate directly to interconnected porosity in basalt when clays and/or other hydrous alteration minerals are present. This apparent porosity excess error is not unknown for sedimentary rocks with hydrous minerals and/or hydrocarbons (Schlumberger Wireline and Testing, 1989). In general, if natural gamma and/or resistivity logs are run in tandem with neutrons logs, these logs can help identify basalt intervals enriched with hydrous minerals. Broglia and Ellis (1990) discussed at length how to employ L_s calculations to correct neutron porosity for alteration mineral effects in oceanic basalts. By doing so, they were able to calculate alteration profiles for the ODP boreholes they studied.

12. Gamma–gamma density logs

A gamma–gamma logging tool actively bombards a borehole with medium-energy gamma radiation and then measures the back-scattered and attenuated gamma flux after it has reacted with the borehole environment. The gamma–gamma log is sometimes called an active gamma log because of the active bombardment by the radioactive source in the tool. Gamma rays with energy between 0.1 and 1 MeV interact with orbital electrons through Compton scattering collisions. Gamma rays lose some of their energy with each Compton scattering event. This attenuation of the active gamma flux is a function of the electron density, and for most rocks, including basalt, electron density is linearly proportional to bulk density. Gamma rays which reach lower energies (< 150 keV) are subject to both Compton scattering and to outright absorption. Absorption depends on the photoelectric cross section, which is inversely related to gamma energy and is directly related to the average atomic number of the medium.

Properly calibrated and corrected gamma–gamma logs can yield accurate and precise measurement of bulk density in a wide range of lithologies. High gamma flux means low density, and vice versa. The utility and popularity of this log for density determination is the reason it is commonly referred to as a density log or gamma–gamma density log. Photoelectric effect

as an adjunct to the gamma–gamma log is often used in the petroleum industry to correct for the near-field effect of mud pack in a borehole (Schlumberger Wireline and Testing, 1989). Photoelectric effect is also used in geochemical logging, discussed below.

13. Gamma–gamma density logs—basalt applications

The use of the gamma–gamma density log in basalt is no different than in any other rock type. The stratigraphic properties of basalt which are sensitive to changes in bulk density are both compositional and textural. Intraflow features are mostly textural, like changes in vesicularity. The vesicular flow tops and bottoms of basalt are less dense than compact and massive flow interiors. The largest density differences, however, are usually between flows and interbeds, the result of both the compositional and textural changes between basalt and most sedimentary rocks.

14. Gamma–gamma density logs—results and interpretations

Fig. 6 shows both the gamma–gamma density and epithermal neutron logs for well 2-2A at the INEEL. Stratigraphy for this well is based on examination of 2-2A cores. Intraflow density changes in basalt are measurable within most flows, grading from less-dense vesicular basalt at flow boundaries to denser massive basalt in flow interiors (see Fig. 6, feature A). Furthermore, the density contrast of basalt vs. interbed is usually greater than the intraflow density contrast (Fig. 6, feature B). Overall, the density contrast between the interbeds and the flows on Fig. 6 is sufficient to identify flow and interbed boundaries. Combining the gamma–gamma density log with a neutron log makes these boundaries even more apparent.

Large voids like collapsed lava tubes can show up on the gamma–gamma density log for the same reasons they show up on the natural gamma log: there are no significant particle interactions in void spaces. On a density log, this results in less gamma flux attenuation. When logging, depth intervals with high counts on the gamma–gamma density log should be re-examined on other logs, such as the natural gamma
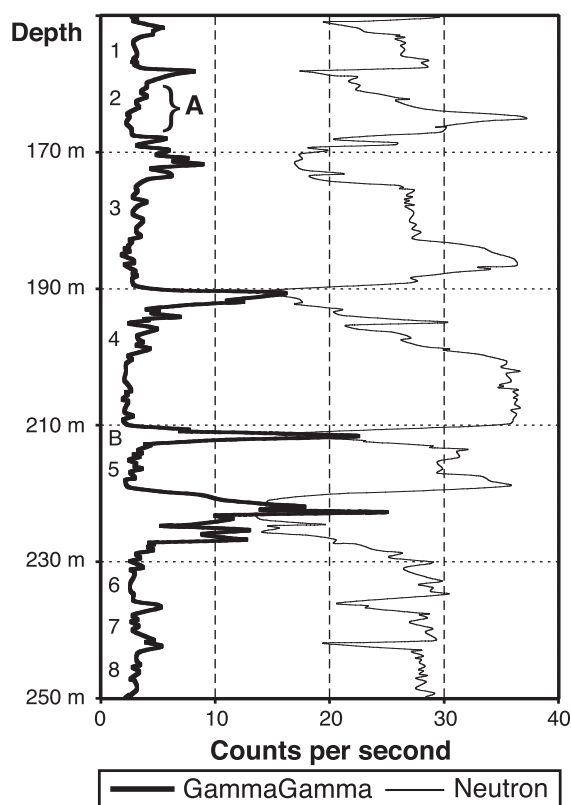
Fig. 6. Gamma–gamma density (left) and neutron (right) logs collected by the USGS in 1978 (Scott et al., 1979) from INEEL well 2-2A on the Eastern Snake River Plain. Well 2-2A is likely the most studied borehole on the East Snake River Plain, with multiple logs available of drill cuttings and core, plus an extensive suite of wireline logs. Individual basalt flows are numbered down the left margin of the figure. Feature A—the signature of a basalt flow grading from a more porous flow top to a dense massive flow interior, characterized by decreasing gamma flux on the gamma–gamma density log, indicating increase in density, plus increasing neutron flux, indicating decreasing porosity and/or hydrous minerals. Feature B—signature of an interbed, with elevated gamma flux on the gamma–gamma density, indicating decreased density, and low neutron counts, indicating increased porosity and/or hydrous minerals.

and caliper logs, for evidence of possible voids. In Fig. 7, suspected voids (shaded intervals) in INEEL well C1A are characterized by local maxima on the gamma–gamma density log (i.e., by very little gamma flux attenuation), indicative of lowered density. Corresponding minima on the natural gamma log support that these gamma flux peaks on the gamma–gamma density log are caused by a textural and not a compositional density drop. These log responses

correlate to two intervals of extensively fractured basalt and basalt rubble in the C1A cores archived by the United States Geological Survey (USGS).

15. Gamma–gamma density logs—problems of interpretation

The attenuated gamma flux of a gamma–gamma density tool below the water table is significant when compared to the attenuated flux in the unsaturated zone, and this must be accounted for when correcting a gamma–gamma log for borehole diameter and other physical variables before attempting any quantitative analysis for bulk density.

16. Geochemical logs

Geochemical logging is performed using nuclear tool combinations incorporating various neutron and gamma-ray sources, coupled with a variety of passive and activated gamma spectrum detectors. Measuring the gamma energy spectrum is the backbone of geochemical logging techniques. Since both passive gamma spectra and activated gamma spectra can be resolved for emission contributions from discrete elements, it is possible for a combination of tools to measure relative major and trace element concentrations at depth. For example, a neutron–gamma log measures the gamma-ray emissions caused by the capture of thermal neutrons. Each element that can capture a thermal neutron will emit gamma rays with characteristic energies specific for that element, notably Ca, Cl, Fe, H, S, and Si (Hertzog et al., 1988; Lamont-Doherty Earth Observatory, 2001). A variant of neutron–gamma logging measures prompt gamma emissions caused instead by the inelastic collision of fast neutrons with certain elements, namely, Ca, C, Fe, O, S, and Si (Hertzog et al., 1988; Lamont-Doherty Earth Observatory, 2001). K, Th, and U concentrations can be determined by measuring the natural gamma energy spectrum. The variety of source and detector combinations is quite large and describing them all is beyond the scope of this study.

Through the use of a proprietary analysis technique, Schlumberger developed a means to measure
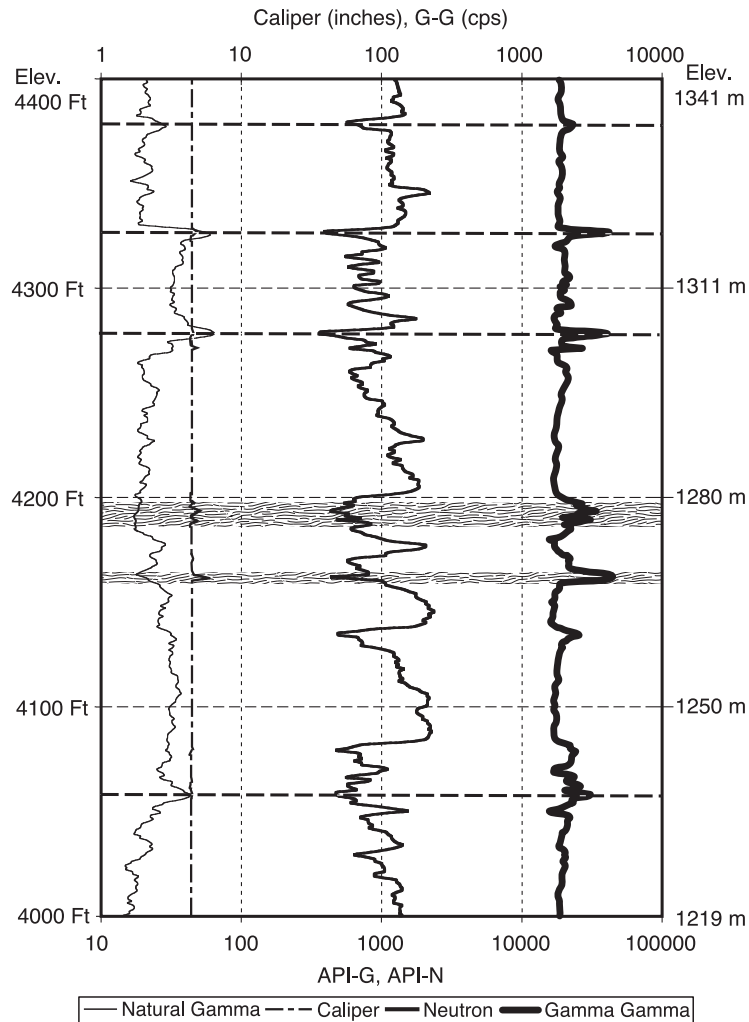
Fig. 7. Signature of void space in basalt for INEEL well C1A on the Eastern Snake River Plain. The caliper tool shows that the borehole has widened in the hatched intervals. The combination of lowered neutron flux plus lowered natural gamma counts argues that water in pores and fractures is the cause of the attenuated neutron flux, and not the presence of hydrous minerals. The combination of decreased gamma counts on the natural gamma log and increased gamma flux on the gamma–gamma density log indicates a decrease in density. C1A cores show that the hatched intervals are zones of fractured basalt and basalt rubble.

elemental abundances quantitatively in the 1980s. By adding a gamma–gamma density log to measure electron density and photoelectric capture cross section (PEF), Mg concentration can be determined from the difference between the measured and calculated PEF based on the directly measured major elements concentrations. Once all relative concentrations have been measured or calculated, this information can be incorporated into an oxide-closure model to deter- mine abundances of major and trace elements, in- cluding K, Ca, Mg, Na, Fe, S, Ti, Si, Al, U, Th, and Gd (Herron and Herron, 1990; Hertzog et al.,1986; Hertzog et al., 1987). Schlumberger's proprietary method was originally developed for use in sedimen- tary rocks for petroleum exploration purposes, and the original oxide-closure models were based on elemental abundances representative of sedimentary environments.

17. Geochemical logs—basalt applications

The composition of basalt varies vertically between flow groups (Wetmore, 1998) much more than it varies laterally (cf. Bates, 1999). Geochemical logs can discriminate, therefore, between flow groups and can correlate flow groups between boreholes. Spectral neutron–gamma logging has been used successfully and extensively at the Pacific Northwest National Laboratory (PNNL) in Washington State, in order to characterize both rocks and contaminants in the sub-surface at the PNNL, in both sediments and Columbia River basalts (Last and Horton, 2000). Access to these spectral neutron–gamma logs is limited, however, since much of the PNNL data is published only in PNNL internal documents.

The sedimentary-rock-based calibrations and oxide-closure model originally developed for Schlumberger's geochemical method are precise though not accurate for several major elements when tested in basalt by the ODP and closely related studies (Brewer et al., 1989, 1990; Anderson et al., 1990a). Subsequently, successful calibrations and oxide-closure models were developed for geochemical logging in oceanic basalts as well as in other crystalline rocks (Anderson et al., 1990a,b; Brewer et al., 1990; Draxler, 1990).

18. Geochemical logs—results and interpretations

The ODP and other researchers have demonstrated the usefulness of oxide-closure models for geochemical logging in the oceanic environment and in continental mafic rocks using Schlumberger's original suite of geochemical tools. Anderson et al. (1990b) have demonstrated that their basalt-specific geochemical log calibration and oxide-closure model gave acceptable results in a small number of boreholes dominated by continental mafic rocks in saturated conditions. Though some studies like Bates (1999) show that intraflow features in continental basalt flows can have variable composition, most basalt flows and flow groups do not vary significantly in composition laterally (e.g., Buckley and Oliver, 1990; Hooper, 1997; Hughes et al., 2002). It is clear, therefore, that even the most complex geochemical tool suites can be properly calibrated for basalt, and

should be able to distinguish between basalt flow groups and interbeds by composition alone. Anderson et al. (1990a,b) and Brewer et al. (1990) have published detailed studies and reviews of geochemical logging in mafic igneous rocks.

19. Geochemical logs—problems of interpretation

Neutron–gamma tools behave very differently above the water table compared to below, as was demonstrated by Crosby and Anderson (1971); this effect is largely due to variations in L_s in saturated vs. unsaturated conditions. Below the water table, L_s is dominated by H, while above the water table, L_s is much larger and more variable due to changes in lithology. Since spectral neutron–gamma logs are a very important component of geochemical logging (Hertzog et al., 1987; Herron and Herron, 1990), tool calibrations and oxide-closure models should be developed for unsaturated basalts. To date we know of no basalt-specific calibrations and oxide-closure models available for unsaturated basalts.

Many geochemical wireline techniques can deliver qualitative elemental concentration measurements in basalt. Quantitative results are possible but depend on using tool calibrations which are appropriate for mafic rocks. There are no tools "off-the-shelf" calibrated for both saturated and unsaturated basalt. Geochemical tools and methods that are capable of measuring quantitative elemental abundances in basalt have been either specialized for use in very limited conditions, like at PNNL, or are proprietary petroleum-exploration technology with a large price tag attached. In addition, Schlumberger's original geochemical tools have been replaced by a second-generation tool suite which utilizes recent advancements in germanium detectors. Though the Schlumberger tools and oxide-closure method can deliver the most versatile and accurate results, the new generation of tools would require recalibration and a new oxide-closure model before they could be deployed. Geochemical logging in basalt is currently limited by equipment and calibration issues, but this technique alone has the potential to resolve basalt flow stratigraphy at the scale of individual flows, without supplement from other wireline tools.

20. Resistivity logs

Resistivity is essentially the inverse of conductivity. Most rock types are resistant to electric currents. On the other hand, water is conductive compared to most earth materials, so when water is present in a rock, it will dominate any resistivity measurements. Assuming that resistivity response is a measure of water content, then resistivity in porous rocks can be treated as a function of water-filled porosity, where the correlation equation between resistivity and water-filled porosity is Archie's Law (Schlumberger Wireline and Testing, 1989). Resistivity is also useful in stratigraphic studies (e.g., Versey and Singh, 1982) since different lithologies have differing resistivities. In addition, it is often possible to use resistivity to identify thin zones of increased permeability: since permeable zones have higher water content in saturated strata, it is often possible to identify these zones by comparing the response of closely spaced "near" electrodes vs. more-separated "far" electrodes, where the former will show a disproportionate decrease in conductivity compared to the latter (Goldberg, 1997).

21. Resistivity logs—basalt applications

Saturated basalt flows have a characteristic response on resistivity logs (e.g., Versey and Singh, 1982; Buckley and Oliver, 1990; Pezard, 1990). In general, resistivity is very high in the massive interiors of basalt flows and low at flow breaks and in interbeds. This behavior is due to both porosity and compositional changes between flows and interbeds. Most interbeds have lower resistivity compared to basalt, since interbed sediments typically include more clays and other conductive minerals and are commonly more porous than most basalts (Lovell and Pezard, 1990). Intraflow resistivity variations are governed mostly by porosity changes. Flow interiors tend to have much lower porosity than flow boundaries, so the amount of conductive fluid present is low and resistivity is high. Depending on the conductive fluid, the uncorrected resistivity of flow interiors is usually greater than 1000 Ω m. Hence, a lateral or long/short normal resistivity tool is preferred over an induction tool in basalt, since many of the former can handle the extremely high resistivities encountered in the massive

interiors of basalt flows whereas most commercially available induction tools cannot (Goldberg, 1997).

22. Resistivity logs—results and interpretation

Fig. 8 shows the lateral resistivity log for the first 250 m of the Hawaii Scientific Drilling Project (HSDP) pilot hole, KP-1 (International Continental Drilling Program, 1999). KP-1 was continuously cored; photographs and an annotated lithological log of the complete core suite are archived at the HSDP web pages at the California Institute of Technology (Hawaii Scientific Drilling Project, 1993). The flows, flow breaks, and interbeds shown in Fig. 8 are based on the lithological logs and unit descriptions from the Hawaii Scientific Drilling Project (1993), Stolper et al. (1996), and Beeson et al. (1996). The KP-1 pilot hole was drilled through the distal aprons of the Mauna Loa and Mauna Kea shield volcanoes where the two overlap. The drilling site was immediately adjacent to the shoreline, and the water level in the hole was ~ 30 m bls when the hole was logged. There is no wireline data for the unsaturated zone of KP-1. The KP-1 resistivity log shows a typical wireline behavior for a saturated basalt flow sequence: the resistivity is high in the middle of flows, and low at flow breaks and interbeds.

Fig. 9 shows long/short normal resistivity logs for INEEL well C1A on East Snake River Plain, for depths 0 to 400 m bls. The conductive fluid in the saturated basalts was potable water from the Snake River Plain aquifer. Note that below the water table at 180 m, the resistivity data show the characteristic high-resistivity humps expected in the middle of flows, separated by low-resistivity flow breaks and interbeds. These resistivity features correlate strongly with flows and interbeds observed in the C1A cores. In general, resistivity response below the water table is usually distinctive enough to discern flow stratigraphy (e.g., Pezard, 1990; also see Fig. 8) and can sometimes be used to correlate basalt flows over modest distances (Crosby and Anderson, 1971).

A polymer gel was added to C1A in an attempt to measure resistivity of unsaturated basalt. The resistivity logs do not show the typical response of saturated basalt flows, i.e., resistant flow interiors vs. conductive flow breaks and interbeds. For example, the 64-
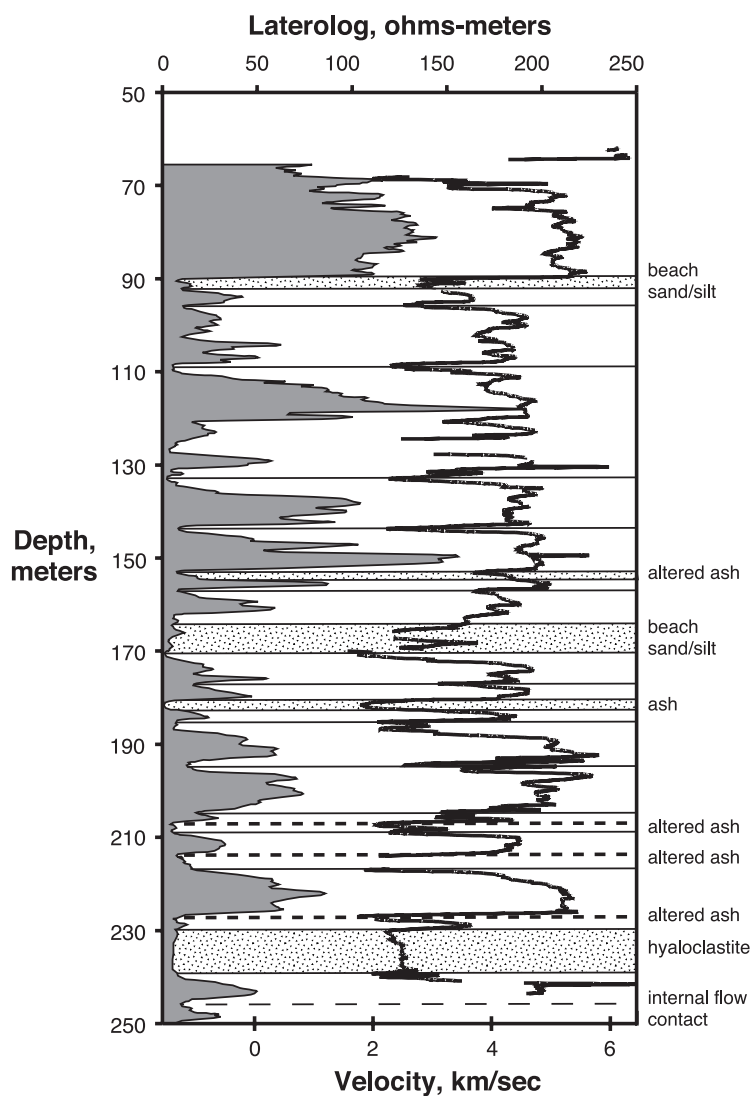
Fig. 8. Lateral resistivity and sonic velocity logs for the HSDP pilot hole KP-1. Both resistivity and velocity increase to the right. Basalt flow interiors are characterized by increased velocity and resistivity, whereas flow breaks are characterized by lowered velocity and resistivity. Data plotted is from the archive of HSDP logging results maintained by the International Continental Drilling Program (International Continental Drilling Program, 1999). Lithology based on cores is from Stolper et al. (1996) and Beeson et al. (1996).

in. (162.6 cm) long normal resistivity log is significantly different from the 16-in. (40.6 cm) short normal resistivity log at depths between ∼ 40 and ∼ 75 m bls, and again at ∼ 175 m bls. One viable explanation is that the resistivity behavior is indicative of resistivity reversals, which happen when a layer is thinner than the long electrode spacing but thicker than the short electrode spacing (Schlumberger Wireline and

Testing, 1989). In a resistivity reversal, a resistant thin layer will cause decreasing resistivity on the long normal resistivity log, but increasing resistivity on the short normal resistivity log, causing the two measurements to diverge. Examples of this can be seen in Fig. 9 between 40 and 75 m. Cores from C1A between 40 and 75 m are highly fractured, brecciated, and/or oxidized in layers commonly thinner than 64 in.
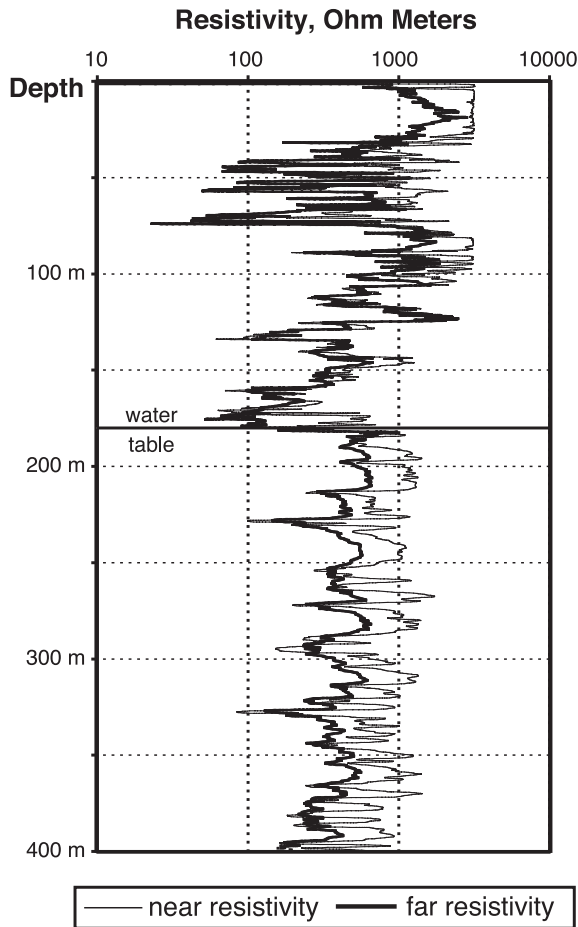
Resistivity, Ohm Meters

Fig. 9. Long and short normal resistivity logs for a portion of INEEL well C1A. Resistivity increases to the right. Electrode spacings are at 64 in. (162.6 cm) and 16 in. (40.6 cm). Depth to the water table is ~180 m bls. Below the water table, the data show the characteristic high-resistivity humps typical of the massive interiors of basalt flows, separated by low-resistivity flow breaks and interbeds. A polymer gel was added to the borehole in the unsaturated zone in order to log resistivity above the water table.

(162.6 cm), so the reversal of the 64-in. (162.6 cm) normal resistivity is possible. Another example of resistivity reversal is shown in Fig. 10, for basalt in INEEL well 2-2A. Though the original researchers at 2-2A collected data for 4-in. (10.2 cm), 8-in. (20.3 cm), 16-in. (40.6 cm), 32-in. (81.3 cm), and 64-in. (162.6 cm) electrode spacings (P. Nelson, pers. comm.), only the 16-in. (40.6 cm) and 64-in. normal resistivity logs (162.6 cm) were published (Scott et al., 1979).

23. Resistivity logs—problems of interpretation

Basalt is one of the most resistive rocks, and many commercially available resistivity tools are inadequate for measuring its extremely high resistivity (e.g., Blackwell et al., 1982; Priest et al., 1982; also see Fig. 9, 0 to 30 m bls). In general, traditional resistivity logs (excluding induction) are not used in dry holes, since resistivity measurements depend on the existence of a closed circuit between electrodes. A closed circuit is usually achieved by the presence of a conductive fluid in the borehole like drilling mud or water. In an air-filled borehole, a closed circuit is not possible since air is not conductive.

There are three potential ways to measure resistivity in unsaturated basalts. The first is to add a conductive fluid, like the polymer gel used in INEEL well C1A. Adding such fluids to a well, however, is often problematic in areas of degraded ground water and heightened regulatory oversight. In addition, such fluids usually break down within hours or days of their injection into a borehole, limiting the window of opportunity to perform resistivity logging. The second way to measure resistivity in a dry hole is to create a circuit by pressing the electrodes against the borehole wall (e.g., Crosby and Anderson, 1971), though in basalt, the frequently uneven nature of the borehole wall may preclude the use of such tools. The third way to log a dry hole would be to use an induction log. Most induction tools are traditionally limited to high-conductivity environments, commonly $<100\ \Omega$ m (Schlumberger Wireline and Testing, 1989), and will not respond in very high-resistivity rocks like basalt (Goldberg, 1997). The experience of the Mt. Hood geothermal project is a good example of the unresponsiveness of an induction tool in basalt flows (Blackwell et al., 1982). In general, a resistivity tool that establishes a physical closed circuit between electrodes is preferred over an induction tool in basalt, since the former can usually handle extremely high resistivity measurements (Goldberg, 1997). Unlike induction tools, however, traditional normal and lateral resistivity tools require the presence of a conductive fluid in the borehole.

Porosity in sedimentary rocks can be calculated from resistivity using Archie's law, but using Archie's law for basalts is problematic (e.g., Becker et al., 1982). It assumes that any contribution by conductive clays is negligible. Using Archie's Law when conduc-
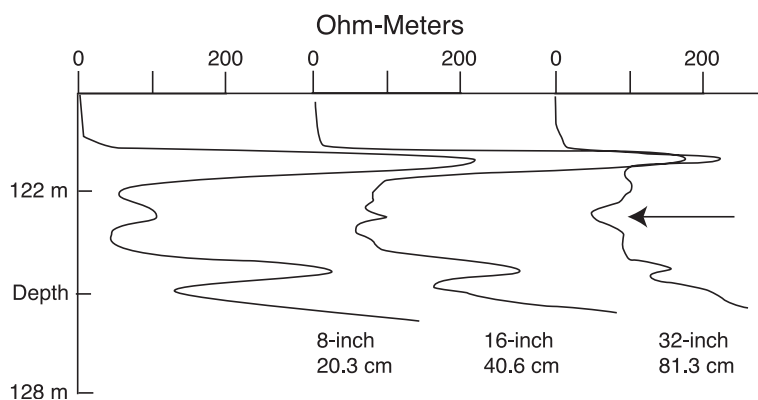
Fig. 10. Three normal resistivity measurements in saturated basalt using electrodes at spacings of 8 (20.3 cm), 16 (40.6 cm) and 32 (81.3 cm) in. The arrow marks the location of a resistivity reversal for a layer less than 32 in. (81.3 cm) thick. This data for INEEL well 2-2A was collected by the USGS in 1978 (P. Nelson, pers. comm.).

tive clay minerals are present can result in porosity calculations which are too high. For rocks with typically low permeability, like amygdaloidal basalt, this juxtaposition of high apparent porosity vs. low permeability is the "apparent porosity paradox" discussed by Pezard (1990) and other DSDP/ODP researchers. There have been attempts to generate valid variations of Archie's Law for basalt (e.g., Pezard, 1990; Becker et al., 1982) to account for alteration and conductivity in cracks and microcracks, with mixed success. Without a good estimate of the concentration and composition of conductive alteration minerals, however, any sort of correction scheme will be doubtful.

24. Velocity logs

Velocity logs, also known as sonic logs or acoustic logs, measure the travel time of an acoustic pulse. Most modern sondes are equipped with one or more pulse transmitters and two or more detectors a short distance away. Two of the principal uses of velocity logs are to calculate porosity and to identify fracture zones (Schlumberger Wireline and Testing, 1989). Fracture zones can be identified by increased travel time for the pulse to reach the detector(s). Porosity can be calculated using the Wyllie time-average equation (Schlumberger Wireline and Testing, 1989; Keys and MacCary, 1971), whose inputs are measured travel time, Δt, and assumed velocities for both the borehole fluid and the rock matrix, V_f and V_m, respectively. Given the mea-

sured Δt for an interval, a reasonable value for porosity can be calculated.

25. Velocity logs—basalt applications

Velocity logs in basalt act no differently than velocity logs in other rocks. There are two items of interest, however, for velocity logs in basalt. The first is the determination of porosity based on measured velocity and travel times. As already discussed, other logs commonly used to calculate porosity, i.e., resistivity and neutron logs, can overestimate porosity when hydrous minerals are present. Velocity logs, however, are independent of neutron moderation and increased conductivity, the properties which introduce an excess porosity error for neutron and resistivity logs, respectively. The porosity derived from velocity logs is the effective porosity, i.e., the interconnected porosity through which fluids can travel. Secondary porosity, i.e., the unconnected pore spaces of unfilled vesicles, vugs, and fractures, is not measured, since the propagating acoustic pulse does not "see" these void spaces, but will travel around them through the solid matrix of the rocks in the borehole (Schlumberger Wireline and Testing, 1989).

The other item of interest is the distinctive pattern of velocity variations made by lower-velocity flow breaks and interbeds which separate higher-velocity flow interiors. This pattern is useful for locating flows, flow breaks, and interbeds in the subsurface.

26. Velocity logs—results and interpretation

Fig. 8 shows a resistivity and velocity log for the KP-1 on Hawaii (International Continental Drilling Program, 1999). Like resistivity, acoustic velocity is high in the massive interior of flows and low at flow breaks and interbeds. Velocity drops in the interbeds and flow breaks due to increased fracturing at flow boundaries and the less cohesive nature of the interbeds compared to flow interiors. This pattern of velocity variation seems to be present in most basalt flow sequences where velocity logs have been collected.

27. Velocity logs—problems of interpretation

A fracture zone in the interior of a flow cannot be distinguished from a flow break by using a velocity log alone, since both phenomenon will cause increased travel times for the acoustic pulse. If a fracture zone is not infilled with sediment, then it may be possible to correctly identify it if the natural gamma log is constant through the zone in question. If the fracture zone is unaltered and/or unsaturated, then magnetic susceptibility and neutron logs will also be constant through the fractured interval.

28. Magnetic susceptibility logs

When any material is exposed to a magnetic field H, it acquires an induced magnetization J (following the symbol and unit conventions of Butler, 1992). The magnitude of J is related to the applied field H by a dimensionless proportionality constant, χ, known as the magnetic susceptibility, such that $J = \chi H$. Magnetic susceptibility is essentially a measure of how strongly a material can be magnetized (Butler, 1992; Dunlop and Ozdemir, 1997). In borehole geophysics, magnetic susceptibility is measured on a volume basis (e.g., Nelson, 1993). The units for χ are dimensionless and are commonly reported as μSI, mSI, or SI units. Units of μSI are most common since the magnetic susceptibility of most earth materials is $\sim 10^{-6}$ SI (Dean, 1995).

Magnetic susceptibilities for the ferromagnetic minerals, i.e., minerals which can carry remanent magnetization, are greater by several orders of magnitude than most other earth materials (Butler, 1992;

Dean, 1995). When present, ferromagnetic minerals will dominate the magnetic susceptibility of any rock. For this reason, magnetic susceptibility tools are designed and calibrated for use in rocks containing ferromagnetic minerals. This is actually of great utility since some of the most common rock-forming minerals are ferromagnetic, including magnetite and hematite. Goethite and hematite typically have magnetic susceptibilities less than 100 μSI, though in some cases, χ can be as high as 250 μSI for goethite and as high as 1000 μSI for hematite (Clark and Emerson, 1991; Butler, 1992; Dunlop and Ozdemir, 1997). In comparison, the magnetic susceptibility of magnetite ranges from $\sim 10,000$ to $\sim 3,000,000$ μSI (Clark and Emerson, 1991; Dunlop and Ozdemir, 1997).

Magnetic susceptibility in ferromagnetic minerals depends on factors such as magnetic domain size, the amount of titanium substitution for iron, the oxidation history of the magnetic minerals, etc. Dunlop and Ozdemir (1997) present perhaps the most current and comprehensive discussion of factors effecting magnetic susceptibility in minerals. In general, oxidizing magnetite to hematite will cause susceptibility to drop by two or more orders of magnitude, which is not uncommon for weathered soil horizons (Butler, 1992), gossans, or economic mineralization of sedimentary rocks (Scott et al., 1981, 1983). Nelson (1993) reviewed the application of magnetic susceptibility logging in sedimentary rocks and tuffaceous volcanoclastic sequences, noting that in some cases, magnetic susceptibility logs were effective in resolving stratigraphic correlations over ones of kilometers. Fukuma (1998) was able to correlate magnetic susceptibility peaks in oceanic sediments between ODP holes over 50 km apart.

29. Magnetic susceptibility logs—basalt applications

Since magnetite is an important accessory mineral in basalt, basalt is one of the most highly magnetized rocks, with χ values typically greater than 100 μSI. Properties which are sensitive to χ in basalt are both compositional and textural. The initial χ for any given basalt flow is a function of magnetite grain size, which is governed by cooling history, by the amount of magnetite present in the rock, and by the amount of

titanium substitution in the magnetite (Dunlop and Ozdemir, 1997). Post-emplacement changes of χ in basalt are commonly due to the oxidation of magnetite to predominantly hematite plus some ilmenite and other minor oxides (Butler, 1992; Dunlop and Ozdemir, 1997). Secondary stratigraphic features, such as sedimentary interbeds between flows, will typically show up on magnetic susceptibility logs as zones of lowered magnetic susceptibility.

30. Magnetic susceptibility logs—results and interpretation

Fukuma (1998) analyzed magnetic susceptibility in oceanic sediments and submerged, originally subaerial basalts as part of ODP Leg 152, to study the nature of the rifted margin off of southeast Greenland. While there are many ODP and other studies on magnetic susceptibility, Fukuma's (1998) study is a good exam-
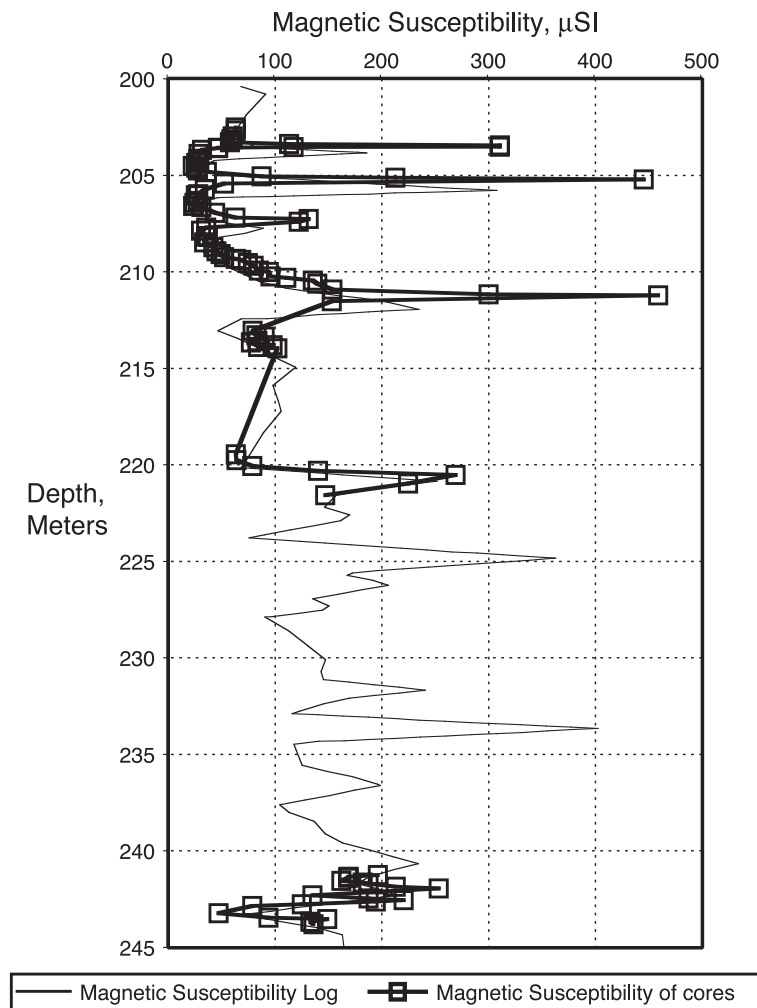

Fig. 11. Magnetic susceptibility log (thin line, no data point markers) collected in the field (Scott et al., 1979) and magnetic susceptibility data (thick line with data point markers) measured on sample cores by the USGS in 1978 (P. Nelson, pers. comm.) for a portion of INEEL well 2-2A on the Eastern Snake River Plain. No depth corrections were applied since it is easier to compare the two data sets with the small depth offset present. The discrepancy exists because the discrete-sample depths were referenced to the ground surface, whereas a hand annotation on the original 1979 paper logs indicates that the log depths were referenced to the top of the well casing, 0.4 m above the ground surface. The complete magnetic susceptibility log for this borehole is shown in Fig. 12.

ple of how several different physical properties can affect the measurement of χ in basalt. The basalts studied by Fukuma behaved as follows: fine-grained scoriaceous basalt at the top of flow units typically had magnetic susceptibilities 2 to 10 times greater (20 to 50 µSI) than basalt flow interiors ($\sim$ 5 to 10 µSI). Some of the fine-grained scoriaceous basalt did not have elevated χ values (< 1 mSI) where it was oxidized. Fukuma (1998) specifically noted that the baseline χ of

flow interiors from different flow series [sic] was controlled by the original composition of unaltered magnetites. Using this information, Fukuma was able to differentiate picritic basalts ($\sim$ 2000 µSI) from more evolved basalts and dacites ($\sim$ 4000 µSI).

Fukuma's (1998) measurements reveal some interesting characteristics of magnetic susceptibility in basalts. Magnetic susceptibility in very fine-grained, quickly cooled scoriaceous flow tops was generally
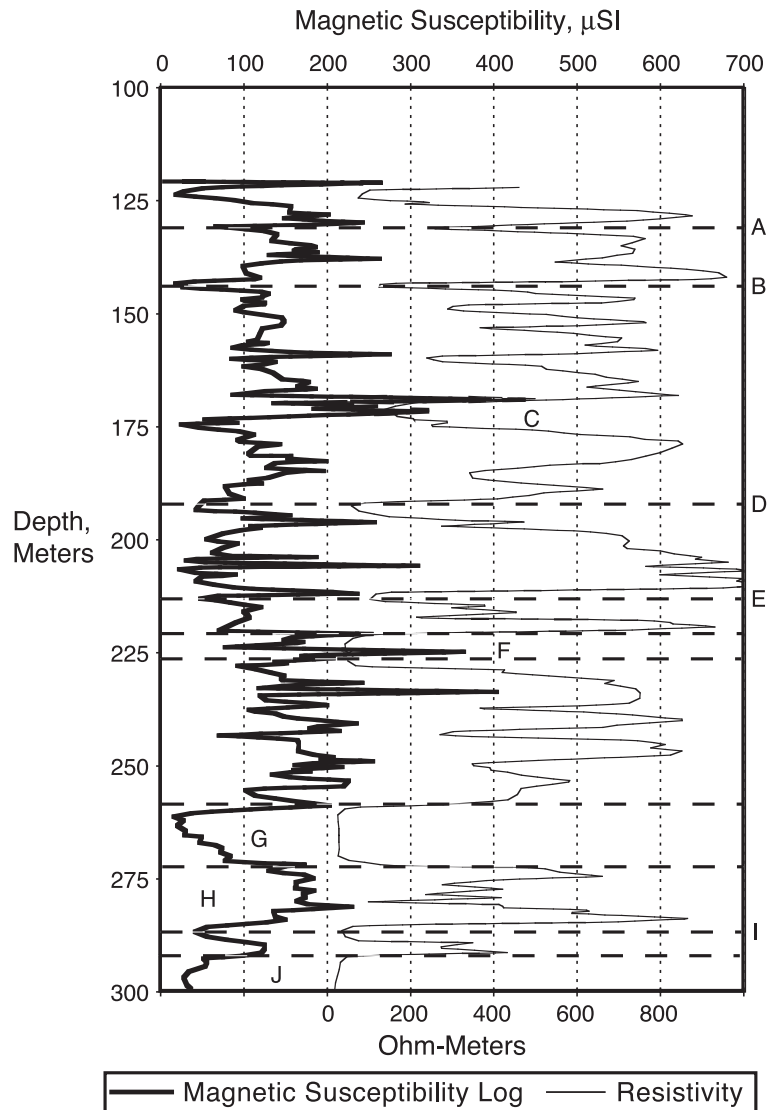

Fig. 12. Magnetic susceptibility and near (16-in./40.6 cm) resistivity logs in basalt for INEEL well 2-2A on the Eastern Snake River Plain (Scott et al., 1979). Lettered features explained in the text.

higher than in flow interiors. This is in keeping with the well-known property of quickly cooled magnetite for preserving magnetic remanence, due to the predominance of small magnetite grains carrying a single magnetic domain (Butler, 1992). The lower magnetic susceptibility of the flow interiors can be interpreted as the consequence of longer cooling times, leading to larger magnetite grains which carry less-effective multiple magnetic domains (Butler, 1992). Fukuma's (1998) susceptibility results also show that where basalts had been oxidized and ferrous iron minerals were altered to ferric ones, χ dropped typically two orders of magnitude, which is well within the magnetic susceptibility range for hematite. While Fukuma's (1998) measurements were made on discrete sample cores collected during drilling, Fukuma remarked that in situ magnetic susceptibility recorded with a wireline tool would have been preferable and would have had the advantage of delivering a continuous record with no data gaps.

Scott et al. (1979) collected a $\sim$ 200-m magnetic susceptibility log in subsurface sediments and basalts in well 2-2A at the INEEL. They also collected discrete samples from the 2-2A cores which were subsequently measured for magnetic susceptibility in the lab (P. Nelson, pers. comm.). Fig. 11 shows a portion of the magnetic susceptibility log plotted with the susceptibility measurements made on the discrete samples from well 2-2A. Overall, the correlation of the log and the lab measurements is good. Three of the discrete-sample susceptibility peaks are much greater than the corresponding peaks on the continuous log, though the lower susceptibility values appear to correlate well. The reason for the mismatch of peaks is not known, though it may be the consequence of different susceptibility bridge configurations used in the lab and the field, different sample volumes, or a bad calibration of either the wireline tool or the laboratory susceptibility bridge. The depth interval plotted on Fig. 11 is a subset of the magnetic susceptibility log for well 2-2A shown in Fig. 12.

31. Magnetic susceptibility—potential problems of interpretation

Fig. 12 shows the magnetic susceptibility log and the 16-in. (40.6 cm) resistivity log collected by Scott

et al. (1979). It is quickly apparent that there is more detail in the magnetic susceptibility log than can be correlated with details on the resistivity log. This is due to the fact that variations in magnetic susceptibility do not always reflect primary compositional or textural features such as flow breaks or magnetite abundance. This can be shown by correlating the lithology of well 2-2A cores to features on the logs (Doherty, 1979; Blair, 2002; Anon., unpubl. data, 1978–2002, archived at INEEL HDR).

Features A, B, D, E, and I mark the location of thin sedimentary interbeds characterized by low resistivity. Each of these is also associated with decreased magnetic susceptibility, indicative that there are either no ferromagnetic minerals present, or that any magnetic minerals present are highly oxidized. In general, flow interiors have background magnetic susceptibilities an order of magnitude greater than those of the thin interbeds. Features G and J are thick sequences of silty clay, both with lowered resistivity and magnetic susceptibility. This interbed pattern, however, is not consistent; for example, feature F is an interbed layer of both silty clay and sand. Feature C is a wide layer of lowered resistivity, but with several magnetic susceptibility peaks. The lithological log of the borehole (Doherty, 1979) describes the region from 143 to 192 m as one flow group with six individual flows and no interbeds. The basalt of the flow group is logged as highly fractured. Above feature C, the upper four flows are described as being oxidized and discolored with "iron-oxide staining." The flows below C are still highly fractured but are not described as being oxidized or altered. Overall, the flow breaks correspond to regions of higher magnetic susceptibility and lowered resistivity. At feature C, the basalt is fractured and hosts two closely spaced flow breaks. The magnetic susceptibility peaks may represent quickly cooled fine-grained basalt at flow tops and bottoms, similar to the flow margins examined by Fukuma (1998), and/or tool response artifacts due to thinly bedded and fractured flows (Nelson, 1993).

Feature H on Fig. 12 is similar to the situation at C; however, the flow group here not only hosts several individual flows, but also four very thin silty clay interbeds (C. Whitaker, pers. comm.; Doherty, 1979). These interbeds show up on the resistivity log much more clearly than on the magnetic susceptibility log. In this case, none of the sedimentary interbeds is associ-

ated with a decrease in susceptibility, arguing that unoxidized ferromagnetic minerals are present, or that the flows and interbeds are thinly bedded. Though the potential for stratigraphic correlation is great (e.g., Fukuma, 1998), magnetic susceptibility logs in basalt should be interpreted in tandem with other log types to identify otherwise confusing intraflow features.

32. Magnetic polarity logs

It is a valid first-order approximation to treat the Earth's magnetic field as a dipole. This dipole is not aligned perfectly with the Earth's rotational axis, but rather wobbles around the rotational axis along a random walk pathway (Butler, 1992). If a remanent magnetization forms quickly in a rock, over a few days or months for most basalts, then all the magnetic moments will point in the direction of the magnetic dipole axis with only a small amount of scatter. If magnetic remanence directions are averaged over periods of 2000 or more years, the averaged direction toward the magnetic dipole axis will be parallel to the Earth's rotational axis. As a tectonic plate moves, remanence directions will point towards the magnetic dipole axis which appears to wander away from the Earth's rotation axis in the reference frame of the tectonic plate. If the layers in a sequence each formed quickly, then the direction of the magnetic moments for any given layer will be approximately the same regardless of where that layer was sampled. It is possible, therefore, to make stratigraphic correlations based on matching remanence directions.

The Earth's magnetic field changes polarity on a scale of 10^5 to 10^6 years. Magnetic remanence records polarity at the time it was acquired. By dating the periods of normal and reversed polarity, it is possible to construct a geomagnetic polarity timescale (GPT). If the pattern of polarity reversals from a sequence of rocks can be matched to a portion of the GPT, then that sequence can be dated paleomagnetically. During a logging program, if a polarity reversal is known or suspected for the rocks in the borehole, it is sometimes possible to map that reversal in the subsurface using a magnetometer tool. Correlating the location of paleomagnetic reversals in boreholes is another powerful paleomagnetic technique for establishing subsurface stratigraphy.

33. Magnetic polarity logs—application and interpretation

There are several different approaches to determine magnetic polarity with a borehole magnetometer. The most rigorous requires a combination of a gyroscopic orientation tool plus a three-component magnetometer (Salisbury et al., 1986). A three-component magnetometer tool contains three orthogonal magnetometers which measure two horizontal and one vertical components. Since all unclamped tools rotate in the borehole, an independent means of determining orientation is required, such as a gyroscopic orientation tool. A magnetometer alone should not be used to determine tool orientation since magnetic anomalies in the borehole can cause deflections in the measured directions.

Once the magnetometer tool has measured magnetization in a borehole, the data must be processed to convert the measurements to a north/east/vertical coordinate system and to remove the effects of the Earth's magnetic field, the induced field of the well casing if present, and the induced field of the rocks and fluids in the borehole (Salisbury et al., 1986). The magnetic susceptibility of the materials in the borehole must be measured or estimated, since without this knowledge, it is impossible to calculate the induced field. Assuming that all the corrections can be made, then the leftover post-correction magnetization should be the remanence, where the polarity is determined by the direction of the vertical component. Salisbury et al. (1986) obtained good results using this methodology on oceanic basalts.

Scott and Olsen (1985) developed a different method for use with a three-component magnetometer. Completely skirting the issue of corrections for the induced field, polarity was estimated based on the deflection of the vertical component of magnetization with respect to true vertical measured with a gyroscope, where positive anomalies correlated with reversed polarity and negative anomalies with normal polarity. Scott and Olsen (1985) obtained good results using this method in volcanic rocks in south central Nevada. This method is similar to that used by Kuehn (1995), who employed a portable fluxgate magnetometer to find polarity reversals in Columbia River Plateau basalts exposed in outcrops.

34. Magnetic polarity logs—potential problems of interpretation

Magnetic polarity logs in basalt are uncommon. While there are many three-component magnetometer tools available for mineral exploration and borehole deviation purposes, there are few tools specifically adapted for magnetic polarity logging in basalt. Some magnetic tools are not adequate for use in strongly magnetized rocks such as basalt, like the Schlumberger-operated specialty tool currently on the OPD ship *Joides Resolution* (D. Goldberg, pers. comm.). Many borehole deviation tools which use magnetometers for orientation may be adaptable for use in basalt, though without the addition of a gyroscopic and/or accelerometer-dependent orientation tool, any magnetic orientations collected in strongly magnetized contiguous basalt flows will be meaningless except for possibly the vertical component.

35. Temperature logs

Temperature logging in boreholes which penetrate continental basalt provides a wide variety of information, including crustal geothermal gradient and heat flow (Blackwell and Steele, 1992), effects of aquifer flow on subsurface temperatures (Ziagos and Blackwell, 1981; Swanberg et al., 1988; Bartolino and Niswonger, 1999), long-term climatic temperature changes (Harris and Chapman, 1997; Pollack et al., 1998; Skinner and Majorowicz, 1999; Majorowicz et al., 1999), and the mechanics of fault zones (Brune et al., 1969; Lachenbruch and Sass, 1980). In addition, Williams and Anderson (1990) reviewed borehole geophysical methods for estimating heat flow in both oceanic and continental basalts in a wide variety of settings.

36. Temperature logs—basalt applications

Temperature logging on the Snake River Plain possibly represents the largest body of work of this type thus far conducted in basalts. This research program has mostly been directed at determination of crustal heat flow and gross characteristics of the Snake River Plain aquifer (Brott et al., 1981; Black-well, 1989). This work has shown that the conductive heat flow is significantly higher than that of the surrounding Basin and Range province and that the rapid movement of cold ground water in Snake River Plain aquifer strongly affects near-surface temperatures and heat flow. In most places boreholes must be several hundred meters deep in order to penetrate beneath the effects of the aquifer and provide a true estimate of the regional conductive gradient and heat flow (see Fig. 13). For such deep wells, temperature profiles show a pronounced inflection at the base of the actively flowing cold waters of the aquifer and allow mapping of the aquifer thickness on parts of the INEEL.

Recent work with temperature logs at INEEL is focused on mapping aquifer temperature variations to define groundwater flow paths. This is possible because temperature of water varies depending on its sources. Much of the aquifer water passing through the INEEL area has been warmed by the high heat flow from the underlying crust to temperatures of 11 to 13 °C. This contrasts sharply with cold recharge water (7 to 9 °C) from drainages north of the Plain, and with anomalously warm zones (up to 18 °C at the water table) where geothermal heat and fluids from depth have affected the aquifer. Current efforts are directed at mapping temperature contours in the aquifer at various depths in an area 100 km by 50 km along the northern boundary of the central Eastern Snake River Plain (R.P. Smith, pers. comm.).

37. Temperature logs—results and interpretations

Work with temperature logs of wells in the East Snake River basalts has produced the following results.

1. The rapidly flowing cold waters of the Snake River Plain aquifer, recharged by high altitude snowmelt, mask the high heat flow of the eastern Snake River Plain. This situation is similar to high-heat flow masking by cold meteoric recharge waters in the actively volcanic Cascade Range described by Swanberg et al. (1988).

2. The aquifer beneath the INEEL ranges in thickness from less than 100 m to about 400 m, similar to aquifer thickness on the Columbia River Plateau in
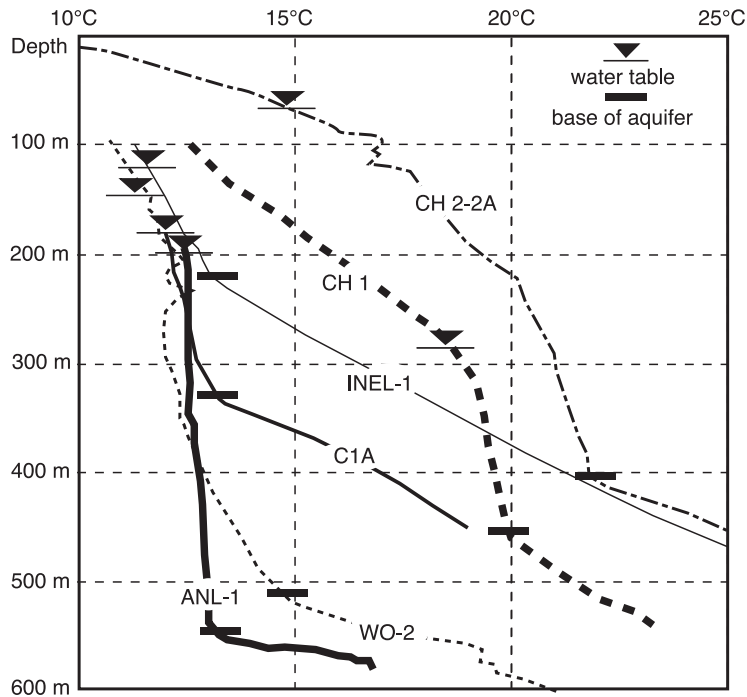
Fig. 13. Temperature profiles of deep wells in basalt flows on the Eastern Snake River Plain. This figure shows typical profiles of temperature gradient above, in, and below the basalt-hosted Snake River Aquifer. Profiles are best exemplified by the temperature log traces for INEEL wells 1 and 2-2a (labeled "CH 1" and "CH 2-2A"). The aquifer corresponds to the portion of the log traces with the lower temperature gradient, and the unsaturated and subaquifer zones by the much higher temperature gradients.

northwestern Washington State (Crosby and Anderson, 1971; Siems, 1973; Siems et al., 1974). Compared to other basalt-hosted aquifers, the Snake River Plain aquifer is one of the thickest basalt-hosted aquifers in the world (cf. Siems, 1973; Cheney and Farr, 1980; Cheney, 1981; Cheney, pers. comm.; Versey and Singh, 1982; Buckley and Oliver, 1990; Hooper, 1997). The thinnest zones in the aquifer correspond to areas where the groundwater is warm and water chemistry indicates long residence time and input of geothermal fluids from depth (Smith et al., 2002).

3. The thickest aquifer zones correspond to areas where the aquifer temperatures remain cool and mostly isothermal to great depths with sharp inflections to the regional high geothermal gradient.

4. Plumes of cold recharge water from local drainages are quickly warmed in some areas and form sharp incursions into warmer aquifer waters in other places.

38. Temperature logs—potential problems of interpretation

Continental basaltic terrains present a unique problem for temperature logging. The extremely porous and permeable nature of the basalts allow easy circulation of fluids (both groundwater and air). In younger basalts, vigorous aquifers commonly form, dramatically affecting heat flow and shallow temperature distributions. In addition, barometric circulation of air to great depths often controls or influences the temperature of rocks above the water table. Because of the temperature effects of these fluids, basaltic terrains are not good candidates for assessment of long-term climatic temperature changes from borehole temperature logs. Also, extremely deep wells are often required for determination of accurate heat flow and regional geothermal gradients.

39. Discussion

39.1. Distinguishing individual layers within a basalt sequence

Determining the depth and thickness of flows, flow groups, and interbeds in a single borehole through a basalt sequence is greatly simplified because of the consistent and characteristic log signature of basalt flow interiors. Flow interiors are the least fractured of all basalt features, so they will have high acoustic velocities; they are aquitards, so their neutron flux will be very high; and they are dense and lack vesicles, so their gamma–gamma counts on a density log will be low. Dense, unfractured, and unaltered basalt is a good electric insulator, so resistivity will be very high for flow interiors. The best logs to identify flow interiors are resistivity and velocity, both of which alone may be sufficient in saturated and subaquifer conditions (e.g., Fig. 8). In unsaturated conditions, neutron logs can sometimes be sufficient to delineate flow interiors (Siems, 1973; Siems et al., 1974), though in some areas like the East Snake River Plain, the neutron log needs to be supplemented by a natural gamma or gamma–gamma log to avoid misinterpretation (e.g., Fig. 6).

Flow tops, flow bottoms, fracture zones, and interbeds are not as easy to distinguish as flow interiors, since these features commonly display variable alteration, water content, fracturing, and density. Fracture zones in basalt will slow velocity and might affect neutron flux depending on the water or clay content, but should not noticeably affect the gamma–gamma counts on a density log because bulk density is relatively unchanged unless large voids spaces are present (e.g., collapsed lava tubes). In comparison, the vesicular tops and bottoms of flows will be less dense and are commonly fractured and oxidized, resulting in decreased bulk density and magnetic susceptibility and significantly degraded velocity (e.g., Bücker et al., 1998). Flow tops and bottoms are also preferred sites for alteration and are commonly the water-bearing zones in saturated conditions, both of which will decrease neutron flux (e.g., Cheney, 1981). Interbeds are less predictable. The typical interbed has a signature of elevated natural gamma counts, low velocity, low resistivity, low neutron flux, and low bulk density. However, while both velocity and neutron flux are almost always low in an interbed, both natural gamma response and bulk density can vary widely depending upon composition and texture.

39.2. Hydrogeological divisions within a basalt sequence

The hydrogeological divisions of a basalt flow sequence can be determined with a minimum of either a temperature or neutron log (see Table 2)—one of the only instances where a single type of log can completely determine the variation in a basalt characteristic for an entire flow sequence.

Table 2
Wireline analyses of hydrogeological zones in basalt flow sequences

Log type	Natural gamma log	Neutron log	Gamma–gamma density log	Temperature log
Unsaturated basalt	Low natural gamma counts in flow interiors, higher elsewhere	Highest neutron flux in flow interiors; moderate neutron flux at flow breaks and interbeds; average flux high	Low gamma flux in flow interiors, higher elsewhere	Positive temperature gradient
Water-saturated basalt (basalt-hosted aquifer)	Uncorrected natural gamma counts attenuated by water, lower compared to unsaturated basalt	Lowest neutron flux in saturated interbeds, flow breaks and fracture zones; moderate to high flux in flow interiors; average flux low	Uncorrected gamma flux attenuated by water, lower compared to unsaturated basalt	Flat temperature gradient through saturation zone
Subaquifer basalt	Generally low natural gamma counts, often indistinguishable from natural gamma response of basalt in the aquifer zone	Low to moderate neutron flux at flow breaks and interbeds; moderate flux in flow interiors; average flux moderate	Low gamma flux in unaltered flow interiors; lowest gamma flux when fractures and vesicles filled w/ alteration minerals	Positive lithostatic temperature gradient

The temperature log can discern the three hydrogeological divisions because of the temperature differences in porous basalt cooled by air and recharge water, porous basalt hosting the aquifer, and impermeable altered basalt subject to the high regional geothermal heat gradient. To see the transition between unsaturated and saturated conditions, the neutron log should be left uncorrected and the log trace should be presented on the same scale above and below the water table, like that for USGS-30 (Fig. 5) as opposed to the scale adjustments by Siems (1973) for Columbia River Plateau basalts (Fig. 4). All of the nuclear logs can distinguish the unsaturated zone/ aquifer boundary because both neutron and gamma fluxes are attenuated by water. Only the neutron log, however, is sensitive to the transition from the saturated to the subaquifer alteration zone because of the contrast in average H content. Neither the natural gamma nor gamma–gamma density logs show sufficient contrast between the saturated and subaquifer alteration zones to distinguish this boundary.

The combination of temperature logs and neutron logs is particularly powerful for mapping water-saturated zones in basalt. Supplementing these with velocity or resistivity logs to locate fracture zones, and fluid resistivity logs to locate changes in water chemistry can greatly refine knowledge of hydraulic conductivity within an aquifer. Flowmeters and fluid resistivity logs were not discussed in this paper, since these behave the same regardless of lithology, but it should be evident that their addition to an aquifer mapping program could greatly enhance the investigation.

39.3. Stratigraphic correlation in a basalt sequence

There are three useful methods for stratigraphic correlations between several boreholes in a basalt sequence, each with different track records. First, a minimum combination of natural gamma, neutron, and gamma–gamma (density) logs should be sufficient to establish basic correlations between boreholes, especially in flood basalts (e.g., Versey and Singh, 1982). When these conventional logs have produced questionable correlations, it is most often because too few tools were used, like natural gamma alone, or that individual features in a borehole were misidentified, as in the case of fracture zones infilled with sediments misidentified as sedimentary interbeds.

Magnetic inclination is a very powerful tool for determining stratigraphy, though it is underutilized in continental basalts. The viability of the overall method, however, has been amply demonstrated by the extensive paleomagnetic studies of cores collected from boreholes on the Snake River Plain (e.g., Champion and Lanphere, 1997; Lanphere et al., 1994; Kuntz et al., 1980). Since magnetic polarity logging has been successful in the past in volcanic rocks (Scott and Olsen, 1985), the only impediment to using this method is the availability of magnetic wireline tools capable in and calibrated for basalt.

Geochemical logging is a powerful tool for stratigraphic correlation (Anderson et al., 1990a,b). The end product of most geochemical logging methods is a qualitative or quantitative estimate of major and some trace element abundances. Natural gamma, gamma–gamma, natural gamma spectroscopy, induced-gamma spectroscopy, and neutron logs have all been used to estimate and correlate various elemental abundances. Several nuclear techniques used in combination should be adequate to correlate flows and interbeds between boreholes.

39.4. Caveats of borehole geophysical logs in basalt

One common problem concerning data analysis in basalt sequences is that one tool alone, rather than a combination of tools, has been used to interpret breaks and internal stratigraphy. For example, natural gamma logs have been used extensively to discriminate flow architecture (e.g., Barraclough et al., 1976; Anderson and Lewis, 1989) and interbeds with elevated natural gamma counts (e.g., Versey and Singh, 1982; Buckley and Oliver, 1990). Basalt flows, however, do not always show sufficient contrast in natural gamma counts to distinguish flows groups (e.g., Cheney, 1981), nor do interbeds always emit higher natural gamma flux (e.g., Quincy diatomite; Siems, 1973). Furthermore, the presence of a natural gamma peak may reflect sediment which has infilled cracks in the interior of a flow, or sediments sandwiched between the former ceiling and floor of a collapsed lava tube. Natural gamma logs need to be interpreted in tandem with other tools, like gamma–gamma and/or neutron logs, which are also sensitive

Table 3
Wireline analyses of basalt flow sequences

Log type	Natural gamma	Neutron	Gamma–gamma density	Resistivity[a]	Velocity[b]	Magnetic susceptibility	Magnetic polarity	Geochemical
Physical basis of measurement	Natural gamma decay of K, Th, U	Scattering and capture of neutrons	Attenuation of active gamma flux by Compton scattering ($\propto$ electron density)	Resistance to electric current	Ease of propagation of acoustic wave	Strength of induced magnetization	Direction of the remanent magnetization vector	A combination of multiple radiation sources plus detectors to measure total and spectral fluxes
Utility for determining basalt stratigraphy	Can distinguish between flow groups. Can distinguish between basalt and interbeds	Can identify flow breaks or interbeds in the unsaturated zone, and fracture zones, flow breaks and/or interbeds below water table	Can distinguish between basalt and interbeds. Can be used to calculated bulk density. Can help identity collapse structures due to decreased density	Can distinguish between flows and flow breaks/interbeds, and between fractured and unfractured basalt	Can distinguish between flows and flow breaks/interbeds	Can distinguish between unaltered basalt and interbeds. Can distinguish between flow interiors and flow margins. Can identify oxidized basalt	Can identify polarity of remanence, help establish geochronology, help distinguish flow groups	Can determine the variation of several major element abundances, to distinguish between flows, flow groups, interbeds and alteration zones
Limitations	Cannot discriminate between basalt and low K/U/TH interbeds, or between flow groups with low K/U/Th contrast	Cannot distinguish between flow breaks, fracture zones or interbeds; or between the effect of water vs. hydrous minerals on neutron flux	Presence of water will attenuate gamma flux	Cannot discriminate between flow breaks and fracture zones; or between conductivity due to water vs. conductivity due to hydrous minerals	Cannot discriminate between fracture zones, flow breaks and interbeds	Cannot discriminate oxidized basalt from other magnetic-mineral bearing rocks	Relatively insensitive to finer stratigraphic details	Level of detail can possibly obscure larger-scale features, elemental abundance determination only as good as the oxide-closure mode used
Sequence-scale features								
Unsaturated basalt	Natural gamma counts generally low in flows, usually higher in most sedimentary interbeds	Highest neutron flux in flow interiors; moderate neutron flux at flow breaks and interbeds	Low gamma flux in flow interiors, higher elsewhere	Highest possible resistivity in flow interiors if resistivity can be measured; lower at flow breaks and interbeds	High velocity, attenuated by fractures and flow breaks, if velocity can be measured	Dominated by ferrous magnetic minerals		

Table 3 (*continued*)

Log type	Natural gamma	Neutron	Gamma–gamma density	Resistivity[a]	Velocity[b]	Magnetic susceptibility	Magnetic polarity	Geochemical
Sequence-scale features								
Water-saturated basalt (basalt-hosted aquifer)	Natural gamma counts always low: uncorrected gamma flux attenuated by water	Lowest neutron flux in saturated interbeds, flow breaks and fracture zones; moderate to high flux in flow interiors	Lower uncorrected gamma flux attenuated by water	High resistivity in flow interiors, lower resistivity at flow breaks	High velocity, attenuated by fractures and flow breaks when present	Potentially lower X from oxidation of ferrous oxides		
Subaquifer basalt	Generally low, often indistinguishable from natural gamma response of basalt in the aquifer zone	Low to moderate neutron flux at flow breaks and interbeds; moderate flux in flow interiors	Low gamma flux in flow interiors without alteration; lowest gamma flux when fractures and vesicles filled w/ alteration minerals	Moderate to high resistivity in flow interiors, lower resistivity at flow breaks	Same or slightly higher velocity, attenuated by fractures and flow breaks when present	Potentially lower X from oxidation of ferrous oxides and growth of alteration minerals	Alteration may reset remanence	
Inter-flow features								
Flow tops and bottoms	Generally lower natural gamma counts than interbeds, higher than flow interiors	Moderate to low neutron flux	Moderate gamma flux, higher than flow interiors	Lower resistivity than flow interiors	Lower velocity than flow interior	Highest X at chilled margin (grain size effect) unless oxidized		
Flow interiors	Lowest natural gamma counts	Highest neutron flux	Lowest gamma flux (highest density)	Highest possible resistivity	Highest possible velocity	High X		Can help correlate flows
Clayey interbed	Highest natural gamma counts since most silts and clays have higher K than basalt	H in unsaturated clay will lower neutron flux compared to unsaturated basalt; saturated basalt may have lower neutron flux than a clayey aquiclude	Variable effect: gamma flux decreases with increasing clay content, positive density error introduced when hydrous minerals are present	Resistivity decrease due to conductive clay minerals	Low velocity	X decreases due to lower ferrous magnetic mineral content and increase in oxidation		Can help correlate interbeds

Feature	Natural gamma	Neutron	Gamma-gamma (density)	Resistivity	Velocity	Magnetic susceptibility (X)	Remanence	Comments
Low-clay interbed	Natural gamma counts usually higher than basalt except in low-K rocks like limestone or diatomite	Neutron flux increases due to greater effective porosity	Gamma flux increases due to decrease in density	Resistivity decrease, especially if comparing the resistivity of flow interiors to interbeds	Low velocity	X decreases due to lower ferrous magnetic mineral content and increase in oxidation		Can help correlate interbeds

Intra-flow features

Feature	Natural gamma	Neutron	Gamma-gamma (density)	Resistivity	Velocity	Magnetic susceptibility (X)	Remanence	
Clay and/or zeolite alteration of basalt	Low natural gamma counts, slight increase compared to unaltered basalt	Lowered neutron flux (excess porosity error)	Low to moderate gamma flux	Lowered resistivity	Little or no increase in velocity compared to basalt Alteration may reset remanence	Lowered X	Attention may reset remanence	
Fracture zones	Variable: large void spaces decrease natural gamma counts; clayey minerals in fractures usually increase natural gamma counts	Low neutron flux in saturated conditions; high to moderate flux in unsaturated conditions, lower if hydrous minerals present	Apparent density drop, gamma flux increases	Usually low resistivity, though variable depending on content and distribution of voids and infilled clays	Usually lower than most flow margins	Variable	Remanence directions may be unreliable in basalt rubble or in basalt disturbed by fracturing	
Collapse structures (lava tubes, etc.)	In general, very low natural gamma counts, lower than most flows		Higher gamma flux			Variable		
Scoria, cinders	Low natural gamma counts		Moderate to high gamma flux			Higher X in unoxidized scoria; lowered X typical of hematite in cinders and oxidized scoria		

[a] Usually used in saturated conditions only, excludes induction logs which are not suitable for basalt.

[b] Usually used in saturated conditions only.

to flow architecture. Details on tool combinations that are advisable for wireline logging are presented in Tables 3 and 4, which summarize the physical prop-

Table 4
Effective wireline tools in basalt

Basalt property or characteristic	Effective tools and tool combinations
Mineral and elemental composition	
K, Th, U	Natural gamma, natural gamma spectroscopy, geochemical
Magnetic minerals	Magnetic susceptibility
Ca, Cl, Fe, H, S, and Si	Neutron-spectral gamma—capture mode
Ca, C, Fe, O, S, and Si	Neutron-spectral gamma—inelastic mode
K, Si, Ca, Fe, S, Ti, Al, U, Th, Gd, Mg	Natural gamma, neutron, magnetic susceptibility, natural spectral gamma, neutron–spectral gamma, gamma–gamma density w/PEF, geochemical
Stratigraphic features	
Location and thickness of flow interiors	Any combination of very high resistivity[a], high velocity[b], high neutron flux, low gamma flux on gamma–gamma density log
Correlation of basalts flows between boreholes	Magnetic polarity and/or geochemical (including natural gamma)
Paleomagnetic geochronology	Combination of magnetic polarity, magnetic susceptibility, gyroscope
Aquifer thickness	Combination of low neutron + low/no temperature gradient
Intra-flow features	
Fracture zones with no sediment infilling	Combinations of attenuated or no velocity[b], extremely low natural gamma counts, high gamma flux on gamma–gamma density log, large variable caliper, low neutron flux in saturated conditions
Fracture zones with sediment infilling	Combinations of attenuated or no velocity[b], large variable caliper, low neutron flux in saturated conditions, decreased gamma flux on gamma–gamma density log
Hydrous alteration minerals	Combination of low neutron + elevated natural gamma, or of low neutron + increased gamma flux on gamma–gamma density log
Collapse structures	Combination of extremely low natural gamma counts, high gamma flux on gamma–gamma density log, large caliper measurements

[a] Usually used in saturated conditions only, induction logs not recommended.
[b] Usually used in saturated conditions only.

erties measured by most of the tools discussed and how these properties vary stratigraphically in continental basalt sequences.

Porosity is probably the most difficult physical parameter to determine in basalt. Every study reviewed here that has used neutron logs in basalt has noted a positive error in saturated porosity introduced by hydrous clay or zeolite minerals. In resistivity logging, these hydrous minerals also introduce a positive error in effective porosity, even when using a highly modified basalt-specific Archie's Law. When hydrous minerals are present, their contribution to neutron and resistivity logs cannot be quantitatively determined unless corrected for using a method like that developed by Broglia and Ellis (1990). For this reason, traditional wireline logs in basalt should be expressed in terms of the physical parameters which are directly measured by each tool, not in terms of calculated or inferred parameters like density or porosity. Reporting tool response in terms of uncorrected physical parameters is also useful for identifying the hydrogeological divisions within a basalt flow sequence (e.g., saturated vs. unsaturated), with the caveat that the saturated and unsaturated response of most tools may be irreconcilable if the tools have not been carefully calibrated for both environments.

40. Conclusion

Interpreting borehole geophysical logs from basalt requires a fundamental understanding of both the tool and basalt volcanology. Data should be measured in terms of what each wireline tool actually measures, and not in terms of the physical properties a tool is assumed to measure in the sedimentary environment. Table 3 summarizes the tools discussed in this paper, the actual property measured by each tool and the stratigraphic features it is sensitive to in a continental basalt sequence. We have found that in basalt provinces with substantial unsaturated zones, it is often useful not to correct for the presence of fluid in the borehole, but rather to use the uncorrected logs to help map aquifers, and to identify zone of higher hydraulic conductivity within aquifers. Determining porosity is perhaps the most problematic issue in applying borehole geophysical methods in basalt, and in general, neutron and resistivity logs should be used cautiously

for this purpose because of the difficulty in identifying and compensating for the error introduced by hydrous minerals like clays and zeolites.

The success of a borehole geophysical investigation to determine stratigraphy will depend on selecting an appropriate combination of tools to measure properties appropriate for basalt. Geochemical and magnetic polarity logging are two of the most powerful methods for determining stratigraphic features in basalt sequences, though less common than using several standard and easily available tools in combination. Determining a comprehensive stratigraphic sequence in basalt can be done with a minimum of five commonly available tools: natural gamma, neutron, velocity, resistivity, and gamma–gamma density. Neutron, gamma–gamma density, resistivity, and velocity tools will locate the flow interiors. The intelligent comparison of natural gamma, neutron, velocity, and gamma–gamma density logs should identify fracture zones, flow tops and bottoms, and most interbeds. Natural gamma, gamma–gamma density, and caliper logs should suffice to identify any collapsed structures still harboring void spaces. Upgrading to a natural gamma spectrum tool and adding magnetic susceptibility will enhance and refine the details of the stratigraphic column.

Acknowledgements

References

Anderson, S.R., Bartholomay, R.C., 1995. Use of natural-gamma logs and cores for determining stratigraphic relations of basalt and sediment at the Radioactive Waste Management Complex, Idaho National Engineering Laboratory, Idaho. J. Idaho Acad. Sci. 31 (1), 1–10.

Anderson, S.R., Lewis, B.D., 1989. Stratigraphy of the Unsaturated Zone at the Radioactive Waste Management Complex. Idaho National Engineering Laboratory, Idaho. U.S. Geol. Survey Water-Resources Investigations Report 89-4065. 54 pp.

Anderson, R.N., Honnorez, J., Becker, K., Adamson, A.C., Alt, J.C., Emmermann, R., Kempton, P.D., Kinoshita, H., Laverne, C., Mattl, M.J., Newmark, R.L., 1982. DSDP Hole 504B, the reference section over 1 km through layer 2 of the oceanic crust. Nature 300, 589–594.

Anderson, R.N., Dove, R.E., Preston, E., 1990a. Geochemical well logs: calibration and lithostratigraphy in basaltic, granitic and metamorphic rocks. In: Hurst, A., Lovell, M.A., Morton, A.C. (Eds.), Geological Applications of Wireline Logs. Geol. Soc. London Spec. Publ., vol. 48, pp. 177–194.

Anderson, R.N., Alt, J.C., Malpas, J., Lovell, M.A., Harvey, P.K., Pratson, E.L., 1990b. Geochemical well logging in basalts: the Palisades Sill and the Oceanic Crust of Hole 504B. J. Geophys. Res. 95, 9265–9292.

Bailey, E.H., Irwin, W.P., Jones, D.L., 1964. Franciscan and related rocks, and their significance in the geology of western California. Calif. Div. Mines Geol. Bull., vol. 183. 177 pp.

Barraclough, J.T., Robertson, J.B., Janzer, V.J., 1976. Hydrology of the Solid Waste Burial Ground, as related to the potential migration of radionuclides. Idaho National Engineering Laboratory. U.S. Geol. Survey Open File Report 76-471. 184 pp.

Bartolino, J.R., Niswonger, R.G., 1999. Numerical Simulation Of Vertical Ground-Water Flux of the Rio Grande from Ground-Water Temperature Profiles. Central New Mexico. U.S. Geol. Survey, Water-Resources Investigations Report 99-4212. 45 pp.

Bates, D.L., 1999. The in situ chemical fractionation of an eastern Snake River Plain basalt flow: implications for heterogeneous chemical interaction with groundwater contaminants. Master's Thesis. Idaho State University, Pocatello, Idaho. 146 pp.

Becker, K., Von Herzen, R.P., Francis, T.J.G., Anderson, R.N., Honnorez, J., Adamson, A.C., Alt, J.C., Emmermann, R., Kempton, P.D., Kinoshita, H., Laverne, C., Mattl, M.J., Newmark, R.L., 1982. In situ electrical resistivity and bulk porosity of the oceanic crust Costa Rica Rift. Nature 300, 594–598.

Becker, K., Sakai, H., Adamson, A.C., Alexandrovich, J., Alt, J.C., Anderson, R.N., Bodeau, D., Gable, R., Herzig, P.M., Houghton, S., Ishizuka, H., Kawahata, H., Kinoshito, H., Langseth, M.G., Lovell, M.A., Malpas, J., Masuda, H., Merrill, R.B., Morin,

R.H., Mottl, M.J., Pariso, J.E., Pezard, P., Phillips, J., Sparks, J., Uhlig, S., 1989. Drilling deep into young oceanic crust, Hole 504B, Costa Rica Rift. Rev. Geophys. 27 (1), 79–102.

Beeson, M.H., Clague, D.A., Lockwood, J.P., 1996. Origin and depositional environment of clastic deposits in the Hilo Drill Hole, Hawaii. J. Geophys. Res. 101, 11617–11629.

Belknap, W.B., Dewan, J.T., Kirkpatrick, C.V., Mott, W.E., Pearson, A.J., Rabson, W.R., 1960. API Calibration Facility for Nuclear Logs. American Petroleum Institute Drilling Production, p. 289.

Blackwell, D.D., 1989. Regional implications of heat flow of the Snake River Plain, northwestern United States. Tectonophysics 164, 323–343.

Blackwell, D.D., Steele, J.L., 1992. Geothermal map of North America. DNAG Continent-Scale Map-006. Geol. Soc. of America. Decade of North American Geology series.

Blackwell, D.D., Murphey, C.S., Steele, J.L., 1982. Heat flow and geophysical log analysis for OMF-7A geothermal test well, Mount Hood, Oregon. In: Priest, G.R., Vogt, B.F. (Eds.), Geology and Geothermal Resources of the Mount Hood area. Oregon, State of Oregon Department of Geology and Mineral Industries Special Paper, vol. 14, pp. 47–56.

Blair, J.J., 2002. Sedimentology and Stratigraphy of Sediments of the Big Lost Trough Subsurface from Selected Coreholes at the Idaho National Engineering and Environmental Laboratory, Idaho. Master's Thesis. Idaho State University, Pocatello, Idaho. 148 pp.

Brewer, K., Sakai, H., Adamson, A.C., Alexandrovich, J., Alt, J.C., Anderson, R.N., Bideau, D., Gable, R., Herzig, P.M., Houghton, S., Ishizuka, H., Kawahata, H., Langseth, M.G., Lovell, M.A., Malpas, J., Masuda, H., Merrill, R.B., Morin, R.H., Mottl, M.J., Pariso, J.E., Pezard, P., Phillips, J., Sparks, J., Uhlig, S., 1989. Drilling deep into young ocean crust, Hole 504B, Costa Rica Rift. Rev. Geophys. 27 (1), 79–102.

Brewer, T.S., Lovell, M.A., Harvey, P.K., Pelling, R., Atkin, B.P., Adamson, A., 1990. Preliminary geochemical results from DSDP/ODP Hole 504B: a comparison of core and log data. In: Hurst, A., Lovell, M.A., Morton, A.C. (Eds.), Geological Applications of Wireline Logs. Geol. Soc. London Spec. Publ., vol. 48, pp. 195–202.

Brewer, T.S., Harvey, P.K., Lovell, M.A., Haggas, S., Williamson, G., Pezard, P., 1998. Ocean floor volcanism: constraints from the integration of core and downhole logging measurements. In: Harvey, P.K., Lovell, M.A. (Eds.), Core-Log Integration. Geol. Soc. London Spec. Publ., vol. 136, pp. 341–362.

Broglia, C., Ellis, D., 1990. Effect of alteration, formation absorption, and standoff on the response of the thermal neutron porosity log in Gabbros and Basalts: examples from Deep Sea Drilling Project-Ocean Drilling Program Sites. J. Geophys. Res. 95, 9171–9188.

Brott, C.A., Blackwell, D.D., Ziagos, J.P., 1981. Thermal and tectonic implications of heat flow in the eastern Snake River Plain, Idaho. J. Geophys. Res. 86, 11709–11734.

Brune, J.N., Henyey, T.L., Roy, R.F., 1969. Heat flow, stress, and rate of slip along the San Andreas fault, California. J. Geophys. Res. 74, 3821–3827.

Bücker, C.J., Cashman, K.V., Planke, S., 1998. Physical and magnetic characterization of aa and pahoehoe flows: Hole 990A. In: Larsen, H.C., Duncan, R.A., Allan, J.F., Brooks, K. (Eds.), Proc. ODP, Sci. Results, vol. 163. http://www-odp.tamu.edu/publications/163_SR/chap_05/chap_05.htm (accessed 28 Aug. 2001).

Buckley, D.K., Oliver, D., 1990. Geophysical logging of water exploration boreholes in the Deccan Traps, Central India. In: Hurst, A., Lovell, M.A., Morton, A.C. (Eds.), Geological Applications of Wireline Logs. Geol. Soc. London Spec. Publ., vol. 48, pp. 153–161.

Butler, R.F., 1992. Paleomagnetism Blackwell Scientific Publications, Boston. 319 pp.

Champion, D.E., Lanphere, M.A., 1997. Age and paleomagnetism of basaltic lava flows in corehole ANL-OBS-AQ-014 at Argonne National Laboratory-West. Idaho National Engineering and Environmental Laboratory. U.S. Geol. Survey Open File Report 97-700. 34 pp.

Chase, G.H., Teasdale, W.E., Ralston, D.A., Jenson, R.G., 1964. Completion report for observation wells 1 through 49, 51, 54, 55, 56, 80, and 81 at the National Reactor Testing Station, Idaho. United States Atomic Energy Commission Report IDO-22045-USGS.

Cheney, C.S., 1981. Hydrogeological investigations into the Stromberg Basalts of the Lephepe/Dibete area. Republic of Botswana Dept. of Geol. Survey Report GS10/13. Lobatse.

Cheney, C.S., Farr, J.L., 1980. Results of the borehole geophysical logging, physical properties core analysis and aquifer testing in the Serowe study block. Republic of Botswana Dept. of Geol. Survey GS10 Technical Note No. 7. Lobatse.

Clark, D.A., Emerson, D.W., 1991. Notes on rock magnetization characteristics in applied geophysical studies. Explor. Geophys. 22 (3), 547–555.

Crosby, J.W., Anderson, J.V., 1971. Some applications of geophysical well logging to basalt hydrology. Ground Water 9 (5), 12–20.

Dean, J.A., 1995. Analytical Chemistry Handbook. McGraw-Hill, NYC. 1168 pp.

Doherty, D.J., 1979. Drilling data from exploration well 2-2A, NW 1/4, Sec. 15, T. 5 N., R. 31 E. Idaho National Engineering Laboratory, Butte County, Idaho. United State Geological Survey Open-File Report 79-851. 1 sheet.

Draxler, J.K., 1990. Geochemical Logging Tool (GLT)–Logauswertung in kristallinen Gesteinen. Zentralbl. Geol. Palaeontol. Teil 1, Allgemeine, Angew. 8, 1003–1019.

Dunlop, D.J., Ozdemir, O., 1997. Rock Magnetism. Cambridge Univ. Press, New York, NY. 573 pp.

Ehlers, E.G., Blatt, H., 1982. Petrology: Igneous, Sedimentary and Metamorphic. W.H. Freeman & Co., San Francisco. 732 pp.

Fukuma, K., 1998. 23. Origin and applications of whole-core magnetic susceptibility of sediments and volcanic rocks from Leg152. In: Saunders, A.D., Larsen, H.C., Wise Jr., S.W. (Eds.), Proceedings of the Ocean Drilling Program. Scientific Results, vol. 152, pp. 271–280.

Goldberg, D., 1997. The role of downhole measurements in marine geophysics. Rev. Geophys. 35, 315–342.

Greeley, R., 1982a. The Snake River Plain, Idaho: representative of a new category of volcanism. J. Geophys. Res. 87, 2705–2712.

Greeley, R., 1982b. The style of Basaltic Volcanism in the Eastern Snake River Plain, Idaho. In: Bonnichsen, B., Breckenridge,

R.M. (Eds.), Cenozoic Geology of Idaho. Idaho Bur. Mines Geol. Bull., vol. 26, pp. 407–421.

Greeley, R., King, J.S., 1975. Geologic field guide to the Quaternary volcanics of the south-central Snake River Plain, Idaho. Idaho Bur. Mines Geol. Pam., vol. 160. 49 pp.

Haggas, S.L., Brewer, T.S., Harvey, P.K., 2002. Architecture of the volcanic layer from the Costa Rica Rift, constraints from core-log integration. J. Geophys. Res. 107 (B2), 1–14 (10.1029/2001JB000147, ECV 2).

Harris, R.N., Chapman, D.S., 1997. Borehole temperatures and a baseline for 20th-century global warming estimates. Science 275, 1618–1621.

Hawaii Scientific Drilling Project, 1993.
http://expet.gps.caltech.edu/Hawaii_project.html
(accessed January 28, 2001).

Herron, M.M., Herron, S.L., 1990. Geological applications of geochemical well logging. In: Hurst, A., Lovell, M.A., Morton, A.C. (Eds.), Geological Applications of Wireline Logs. Geol. Soc. London Spec. Publ., vol. 48, pp. 165–175.

Hertzog, R., Soran, P., Schweitzer, J., 1986. Applications of cross section data for nuclear geochemical well logging. J. Radiat. Effects 94, 49–52.

Hertzog, R., Colson, L., Seeman, B., O'Brien, M., Scott, H., McKeon, D., Wraight, P., Grau, J., Schweitzer, J., Herron, M., 1987. Geochemical logging with spectrometry tools. SPE Paper 16792, Transactions Vol. Ω, Formation Evaluation and Reservoir Geology: Soc. of Petroleum Engineers, 447–460.

Hertzog, R., Ellis, D., Grau, J., Schweitzer, J., 1988. Elemental concentrations from gamma ray spectroscopic logs. Nucl. Geophys. 2, 175–182.

Hooper, P.R., 1997. The Columbia River Flood Basalt Province: current status. In: Mahoney, J.J., Coffin, M.F. (Eds.), Large Igneous Provinces: Continental, Oceanic, and Planetary Flood Volcanism. Am. Geophys. Union Monogr., vol. 100, pp. 1–27.

Hughes, S.S., Smith, R.P., Hackett, W.R., Anderson, S.R., 1999. Mafic volcanism and environmental geology of the Eastern Snake River Plain, Idaho. In: Hughes, S.S., Thackray, G.D. (Eds.), Guidebook to the Geology of Eastern Idaho: Idaho Museum of Natural History, Pocatello, ID, USA, pp. 143–168.

Hughes, S.S., McCurry, M., Geist, D.J., 2002. Geochemical correlations and implications for the magmatic evolution of basalt flow groups at the Idaho National Engineering and Environmental Laboratory. In: Link, P.K., Mink, L.L. (Eds.), Geology, Hydrogeology, and Environmental Remediation, Idaho National Engineering and Environmental Laboratory, Eastern Snake River Plain, Idaho. Geol. Soc. Am. Spec. Pap., vol. 353, pp. 151–174.

International Continental Drilling Program/GeoForschungsZentrum-Potsdam, 1999. Hawaii Scientific Drilling Project data. Archived at: http://www.icdp-online.de/sites/hawaii/public/data.html (accessed 24 Feb. 2001).

Keys, W.S., 1990. Borehole geophysics applied to ground-water investigations: techniques of water-resources investigations of the U.S. Geol. Survey, Bk. 2, Chap. E2. 150 pp.

Keys, W.S., MacCary, L.M., 1971. Application of borehole geophysics to water-resources investigations: U.S. Geological Survey Techniques of Water-Resources Investigations, Bk. 2, Chap. E1. 126 pp.

Knutson, C.F., Sullivan, W.H., Dooley, K.J., 1994. Geotechnical logging evaluation of the Eastern Snake River Plain Basalts. Soc. of Prof. Well Log Analysts 34th Annual Logging Symposium, 1–17.

Kuehn, S.C., 1995. The Olympic-Wallowa Lineament, Hite Fault System, and Columbia River Basalt Group Stratigraphy in Northeast Umatilla County. Oregon, Master's Thesis. Washington State University, Pullman, Washington.

Kuntz, M.A., Dalrymple, G.B., Champion, D.E., Doherty, D.J., 1980. Petrography, age, and paleomagnetism of volcanic rocks at the Radioactive Waste Management Complex. Idaho National Engineering Laboratory, Idaho, with an evaluation of potential volcanic hazards. U.S. Geological Survey Open-File Report 80-388. 63 pp.

Lachenbruch, A.H., Sass, J.H., 1980. Heat flow and energetics of the San Andreas fault zone. J. Geophys. Res. 85, 6185–6222.

Lamont-Doherty Earth Observatory, 2001. Geochemical Tool (GLT). Ocean Drilling Program Logging Manual. http://www.ldeo.columbia.edu/BRG/ODP/LOGGING/TOOLS/geochem.html (accessed April 16, 2002).

Lanphere, M.A., Kuntz, M.A., Champion, D.E., 1994. Petrology, age, and paleomagnetism of basaltic lava flows in coreholes at Test Area North (TAN). Idaho National Engineering Laboratory. U. S. Geol. Survey Open File Report 94-686. 49 pp.

Last, G.V., Horton, D.G., 2000. Review of Geophysical Characterization Methods Used at the Hanford Site, PNNL-13149. Pacific Northwest National Laboratory, Richland, WA. 113 pp.

Lovell, M.A., Pezard, P.A., 1990. Electrical properties of basalts from DSDP Hole 504B: a key to the evaluation of pore space morphology. In: Hurst, A., Lovell, M.A., Morton, A.C. (Eds.), Geological Applications of Wireline Logs. Geol. Soc. London Spec. Publ., vol. 48, pp. 339–345.

Macdonald, G.A., 1972. Volcanoes Prentice-Hall. Englewood Cliffs, NJ. 510 pp.

Majorowicz, J.A., Safanda, J., Harris, R.N., Skinner, W.R., 1999. Large ground surface temperature changes of the last three centuries inferred from borehole temperatures in the Southern Canadian Prairies, Saskatchewan. Global Planet. Change 20, 227–241.

Morin, R.H., Barrash, W., Paillet, F.L., Taylor, T.A., 1993. Geophysical logging studies in the Snake River Plain Aquifer at the Idaho National Engineering Laboratory—Wells 44, 45, and 46. U.S. Geol. Survey Water-Resources Investigations Report 92-4184. 44 pp.

Morse, L.H., McCurry, M., 1997. Possible correlations between basalt alteration and the effective base of the Snake River Plain Aquifer at the Idaho National Engineering and Environmental Laboratory. Proceedings of the 32nd Symposium on Engineering Geology and Geotechnical Engineering, held at Boise, Idaho, March 26–28, 1997, 1–13.

Morse, L.H., McCurry, M., 2002. Genesis of alteration of Quaternary basalts within a portion of the eastern Snake River Plain aquifer. In: Link, P.K., Mink, L.L. (Eds.), Geology, Hydrogeology, and Environmental Remediation, Idaho National Engineering and Environmental Laboratory, Eastern Snake River Plain, Idaho. Geol. Soc. Am. Spec. Pap., vol. 353, pp. 213–224.

Nelson, P., 1993. Magnetic susceptibility logs from sedimentary

and volcanic environments. Soc. of Prof. Well Log Analysts 34th Annual Logging Symposium, V1–V15.

Pezard, P.A., 1990. Electrical properties of mid-ocean ridge basalt and implications for the structure of the upper oceanic crust in Hole 504B. J. Geophys. Res. 95, 9237–9266.

Pollack, H.N., Huang, S., Shen, P.-Y., 1998. Climate change record in subsurface temperatures: a global perspective. Science 282, 279–281.

Priest, G.R., Beeson, M.H., Gannett, M.W., Berri, D.A., 1982. Geology, geochemistry, and geothermal resources of the Old Maid Flat area, Oregon. In: Priest, G.R., Vogt, B.F. (Eds.), Geology and Geothermal Resources of the Mount Hood Area, Oregon. State Oreg. Dept. Geol. Miner. Ind. Spec. Pap., vol. 14, pp. 16–30.

Salisbury, M.H., Scott, J.H., Auroux, C., Becker, K., Bosum, W., Broglia, C., Carlson, R., Fisher, A., Gieskes, J., Holmes, M.A., Hoskins, H., Legrand, J., Moos, D., Rio, D., Stephen, R.A., Wilkens, R., 1986. Site 418: Bermuda Rise. Proc., Init. Repts. (Pt. A), ODP 102, 95–149.

Schlumberger Wireline and Testing, 1989. Log Interpretation Principles/Applications Sugarland, Texas. 251 pp.

Scott, J.H., Olsen, G.G., 1985. A three-component borehole magnetometer probe for mineral investigations and geologic research. Soc. Prof. Well Log Analysts 26th Annual Logging Symposium, vol. I, pp. E1–E16.

Scott, J.H., Zablocki, C.J., Clayton, G.H., 1979. Geophysical well-logging data from exploratory Well 2-2A, NW 1/4 Sec. 15, T. 5 N., R. 31 E. Idaho National Engineering Laboratory, Butte County, Idaho, U.S. Geol. Survey Open File Report 79-1460. 1 sheet.

Scott, J.H., Seeley, R.L., Barth, J.J., 1981. A magnetic susceptibility well-logging system for mineral exploration. Soc. Prof. Well Log Analysts 22nd Annual Logging Symposium, vol. II, pp. CC1–CC21.

Scott, J.H., Daniels, J.J., Reynolds, R.L., Seeley, R.L., 1983. Magnetic-susceptibility logging in sedimentary uranium environments. Log Anal. 24 (2), 16–21.

Sharp, R.P., 1976. Field Guide Southern California (Rev. Ed.). Kendall/Hunt Publishing, Dubuque, IA. 208 pp.

Siems, B.A., 1973. Surface to subsurface correlation of Columbia River Basalt using geophysical data, in parts of Adams and Franklin Counties, Washington. Wash. State Univ. Coll. Eng. Bull. 331, 1–65.

Siems, B.A., Bush, J.H., Crosby, J.W., 1974. TiO_2 and geophysical logging criteria for Yakima Basalt correlation, Columbia Plateau. Geol. Soc. Am. Bull. 85, 1061–1068.

Skinner, W.R., Majorowicz, J.A., 1999. Regional climatic warming and associated twentieth century land-cover changes in northwestern North America. Clim. Res. 12, 39–52.

Smith, R.P., Blackwell, D.D., McLing, T.L., 2002. Ground water flow, aquifer geometry, and geothermal interactions inferred from temperature distribution: Snake River Plain aquifer, south-eastern Idaho, Paper No. 42-5. Geol. Soc. Am. Ann. Meet., Abstr. Progr. 34 (6), 96.

Stolper, E.M., DePaolo, D.J., Thomas, D.M., 1996. Introduction of special section: Hawaii Scientific Drilling Project. J. Geophys. Res. 101, 11593–11598.

Swanberg, C.A., Walkey, W.C., Combs, J., 1988. Core hole drilling and the "rain curtain" phenomenon at Newberry volcano, Oregon. J. Geophys. Res. 93, 10163–10173.

Versey, H.R., Singh, B.K., 1982. Groundwater in the Deccan basalts of the Betwa basin, India. J. Hydrol. 58, 276–306.

Walker, G.P.L., 1972. Compound and simple lava flows and flood basalts. Bull. Volcanol. 36, 579–590.

Welhan, J.A., Johannesen, C.M., Reeves, K.S., Clemo, T.M., Glover, J.A., Bosworth, K.W., 2002. Morphology of inflated pahoehoe lavas and spatial architecture of their porous and permeable zones, eastern Snake River Plain, Idaho. In: Link, P.K., Mink, L.L. (Eds.), Geology, Hydrogeology, and Environmental Remediation, Idaho National Engineering and Environmental Laboratory, Eastern Snake River Plain, Idaho. Geol. Soc. Am. Spec. Pap., vol. 353, pp. 135–150.

Wetmore, P.L., 1998. An assessment of physical volcanology and tectonics of the central eastern Snake River Plain based on the correlation of subsurface basalts at and near the Idaho National Engineering and Environmental Laboratory, Idaho, Master's Thesis. Idaho State University, Pocatello, Idaho, 118 pp.

Williams, C.F., Anderson, R.N., 1990. Thermophysical properties of the Earth's crust: in situ measurements from Continental and Ocean Drilling. J. Geophys. Res. 95, 9209–9236.

Ziagos, J.P., Blackwell, D.D., 1981. A model for the effect of horizontal fluid flow in a thin aquifer on temperature-depth profiles. Trans. Geotherm. Resour. Counc. 5, 221–223.